

1      **Nitrogen Fixation in Arctic Coastal Waters**  
2      **(Qeqertarsuaq, West Greenland): Influence of Glacial**  
3      **Melt on Diazotrophs, Nutrient Availability, and**  
4      **Seasonal Blooms**

5      Schlangen Isabell<sup>1</sup>, Leon-Palmero Elizabeth<sup>1,2</sup>, Moser Annabell<sup>1</sup>, Xu Peihang<sup>1</sup>,  
6      Laursen Erik<sup>1</sup>, and Löscher Carolin R.<sup>1,3</sup>

7      <sup>1</sup>Nordceee, Department of Biology, University of Southern Denmark, Campusvej 55, 5230 Odense M,  
8      Denmark

9      <sup>2</sup>Department of Geosciences, Princeton University, Princeton, New Jersey

10      <sup>3</sup>DIAS, University of Southern Denmark, Odense, Denmark

11      **Correspondence:** Carolin R. Löscher (cloescher@biology.sdu.dk)

12      **Abstract.** The Arctic Ocean is undergoing rapid transformation due to climate change, with  
13      decreasing sea ice contributing to a predicted increase in primary productivity. A critical factor  
14      determining future productivity in this region is the availability of nitrogen, a key nutrient that  
15      often limits biological growth in Arctic waters. The fixation of dinitrogen (N<sub>2</sub>) gas, a biological  
16      process mediated by diazotrophs, provides a source of new nitrogen to marine ecosystems and has  
17      been increasingly recognized as a potential contributor to nitrogen supply in the Arctic  
18      Ocean. Historically it was believed to be limited to oligotrophic tropical and subtropical oceans,  
19      Arctic N<sub>2</sub> fixation has only garnered significant attention over the past decade, leaving a gap in  
20      our understanding of its magnitude, the diazotrophic community, and potential environmental  
21      drivers. In this study, we investigated N<sub>2</sub> fixation rates and the diazotrophic community in Arctic  
22      coastal waters, using a combination of isotope labeling, genetic analyses and biogeochemical  
23      profiling, in order to explore its response to glacial meltwater, nutrient availability and its impact  
24      on primary productivity. We observed N<sub>2</sub> fixation rates ranging from 0.16 to 2.71 nmol N L<sup>-1</sup> d<sup>-1</sup>,  
25      notably higher than many previously reported rates for Arctic waters. The diazotrophic community was  
26      predominantly composed of UCYN-A. The highest N<sub>2</sub> fixation rates co-occurred with peaks in  
27      chlorophyll *a* and primary production at a station in the Vaigat Strait, likely influenced by glacial  
28      meltwater input. On average, N<sub>2</sub> fixation contributed 1.6% of the estimated nitrogen requirement of  
29      primary production, indicating that while its role is modest, it may still represent a nitrogen source in  
30      certain conditions. These findings illustrate the potential importance of N<sub>2</sub> fixation in an  
31      environment previously not considered important for this process and provide insights into its  
32      response to the projected melting of the polar ice cover.

**Deleted:** The fixation of dinitrogen (N<sub>2</sub>) gas, a biological process mediated by diazotrophs, not only supplies new nitrogen to the ecosystem but also plays a central role in shaping the biological productivity of the Arctic.

**Deleted:** Here we

**Deleted:** show

**Deleted:** to be

**Deleted:** those observed in many other oceanic regions, suggesting a previously unrecognized significance of N<sub>2</sub> fixation in these high-latitude waters.

**Deleted:** is

**Deleted:** We found

**Deleted:** ing

**Deleted:** maximum

**Deleted:** concentrations

**Deleted:** rates

**Deleted:** close impacted by glacier meltwater inflow, possibly providing otherwise limiting nutrients.

**Deleted:** Our

53

54 

## 1 Introduction

55

56 Nitrogen is a key element for life and often acts as a growth-limiting factor for primary  
 57 productivity (Gruber and Sarmiento, 1997; Gruber, 2004; Gruber and Galloway, 2008). Despite  
 58 nitrogen gas ( $N_2$ ) making up approximately 78% of the atmosphere, it remains inaccessible to most  
 59 marine life forms. Diazotrophs, which are specialized bacteria and archaea, have the ability to  
 60 convert  $N_2$  into biologically available nitrogen, facilitated by the nitrogenase enzyme complex  
 61 carrying out the process of

62 biological nitrogen fixation ( $N_2$  fixation) (Capone and Carpenter (1982)). Despite the fact that these  
 63 organisms are highly specialized and  $N_2$  fixation is energetically demanding, the ability to carry  
 64 out this process is widespread amongst prokaryotes. However, it is controlled by several factors  
 65 such as temperature, light, nutrients and trace metals such as iron and molybdenum (Sohm et al.,  
 66 2011; Tang et al., 2019). Oceanic  $N_2$  fixation is the major source of nitrogen to the marine system  
 67 (Karl et al., 2002; Gruber and Sarmiento, 1997), thus, diazotrophs determine the biological  
 68 productivity of our planet (Falkowski et al. (2008), impact the global carbon cycle and the  
 69 formation of organic matter (Galloway et al., 2004; Zehr and Capone, 2020). Traditionally it has  
 70 been believed that the distribution of diazotrophs was limited to warm and oligotrophic waters  
 71 (Buchanan et al., 2019; Sohm et al., 2011; Luo et al., 2012) until putative diazotrophs were  
 72 identified in the central Arctic Ocean and Baffin Bay (Farnelid et al., 2011; Damm et al., 2010).  
 73 First rate measurements have been reported for the Canadian Arctic by Blais et al. (2012) and  
 74 recent studies have reported rate measurements in adjacent seas (Harding et al., 2018; Sipler et al.,  
 75 2017; Shiozaki et al., 2017, 2018), drawing attention to cold and temperate waters as significant  
 76 contributors to the global nitrogen budget through diverse organisms.

77

JUCYN-A has been described as the dominant active  $N_2$  fixing cyanobacterial diazotroph in arctic  
waters (Harding et al. (2018)), while other cyanobacteria have only occasionally been reported  
 (Díez et al., 2012; Fernández-Méndez et al., 2016; Blais et al.). However, other recent studies  
 suggest, that the majority of the arctic marine diazotrophs are NCDs (non-cyanobacterial  
diazotroph) and those may contribute significantly to  $N_2$  fixation in the Arctic Ocean (Shiozaki et  
 al., 2018; Fernández-Méndez et al., 2016; Harding et al., 2018; Von Friesen and Rie-  
 mann, 2020). Recent work by Robicheau et al. (2023) nearby Baffin Bay, geographically close to the sampling area,  
document low *nifH* gene abundance while still detecting diazotrophs in Arctic surface waters, highlighting  
the patchy distribution of diazotrophs across Arctic coastal environments. Studies on the Arctic  
 diazotroph community remain scarce, leaving Arctic environments poorly understood regarding  
 $N_2$  fixation. Shao et al. (2023) note the impossibility of estimating Arctic  $N_2$  fixation rates due to

87

**Deleted:**  $N_2$  fixation is performed by diverse group of cyanobacteria as well as by non-cyanobacteria diazotrophs (NCDs). ...

**Deleted:** in those waters

**Deleted:** while

**Deleted:** 2012).

**Deleted:** R

**Deleted:** found

**Deleted:**

**Formatted:** Font: Italic

**Deleted:** Still, s

98 the sparse spatial coverage, which currently represents only approximately 1 % of the Arctic  
99 Ocean. Increasing data coverage in future studies will aid in better constraining the contribution  
100 of N<sub>2</sub> fixation to the global oceanic nitrogen budget (Tang et al. (2019)).

101 The Arctic ecosystem is undergoing significant changes driven by rising temperatures and the  
102 accelerated melting of sea ice, a trend predicted to intensify in the future (Arrigo et al., 2008; Hanna  
103 et al., 2008; Haine et al., 2015). These climate-driven shifts have stimulated primary productivity  
104 in the Arctic by 57 % from 1998 to 2018, elevating nutrient demands in the Arctic Ocean (Ardyna  
105 and Arrigo, 2020; Arrigo and van Dijken, 2015; Lewis et al., 2020). This increase is attributed to  
106 prolonged phytoplankton growing seasons and expanding ice-free areas suitable for  
107 phytoplankton growth (Arrigo et al. (2008)). However, despite these dramatic changes, the role of  
108 N<sub>2</sub> fixation in sustaining Arctic primary production remains poorly understood. While recent  
109 studies suggest that diazotrophic activity may contribute to nitrogen inputs in polar regions (Sipler  
110 et al. (2017)), fundamental uncertainties remain regarding the extend, distribution and  
111 environmental drivers of N<sub>2</sub> Fixation in the Arctic Ocean. Specifically, it is unclear whether  
112 increased glacial meltwater input enhances or inhibits N<sub>2</sub> Fixation through changes in nutrient  
113 availability, stratification, and microbial community composition. Thus, the question of whether  
114 nitrogen limitation will emerge as a key factor constraining Arctic primary production under future climate  
115 scenarios remains unresolved. In this study, we investigate the diversity of diazotrophic  
116 communities alongside in situ N<sub>2</sub> fixation rate measurements in Disko Bay (Qeqertarsuaq), a coastal  
117 Arctic system strongly influenced by glacial meltwater input. By linking environmental parameters to N<sub>2</sub>  
118 fixation dynamics, we aim to clarify the role of diazotrophs in Arctic nutrient cycling and assess  
119 their potential contribution to sustaining primary production in a changing Arctic. Understanding  
120 these processes is essential for refining biogeochemical models and predicting ecosystem  
121 responses to future climate change.

## 122 2 Material and methods

### 123 2.1 Seawater sampling

124 The research expedition was conducted from August 16 to 26 in 2022 aboard the Danish military  
125 vessel P540 within the waters of Qeqertarsuaq, located in the western region of Greenland  
126 (Kalaallit Nunaat). Discrete water samples were obtained using a 10 L Niskin bottle, manually  
127 lowered with a hand winch to five distinct depths (surface, 5, 25, 50, and 100 m). A comprehensive  
128 sampling strategy was employed at 10 stations (Fig. 1), covering the surface to a depth of 100 m.  
129 The sampled parameters included water characteristics, such as nutrient concentrations, chl *a*,

**Deleted:** Additionally, t  
**Formatted:** Indent: Left: 0,14 cm, Right: 0,66 cm

**Deleted:** consequent reduc- tion

**Deleted:** in

**Deleted:** extent due to accelerated melting, which is

**Deleted:** increase

**Deleted:** severe

**Deleted:** thereby

**Deleted:** can be

**Deleted:** the extension of the

**Deleted:** the

**Deleted:** sion of

**Deleted:**

**Deleted:** available

**Deleted:** The Greenland Ice Sheet is strongly affected by climate change and the waters of Baffin Bay have experienced a substantial sea surface temperature (SST) increase of 47.4 % along with a significant increase in chlorophyll *a* (Chl *a*) concentration of 26.4 % over the last two decades (1998–2018) (Lewis et al. (2020)). Coastal sites are particularly impacted by melting, receiving glacial runoff enriched with nutrients and trace elements triggering phytoplankton blooms and altering near-shore biogeochemical cycling (Ardyna and Arrigo, 2020; Arrigo et al., 2017; Hendry et al., 2019; Bhatia et al., 2013).

**Deleted:** Given the changes, there is an urgency to explore the role of N<sub>2</sub> fixation in shaping the response of the Arctic ecosystem to these environmental changes. While the general magnitude of N<sub>2</sub> fixation is suspected to have a substantial impact (Sipler et al. (2017)), the complexity of Arctic biogeochemical processes necessitates further studies and broader spatial and temporal investigations to facilitate robust predictions. The question of whether primary

**Deleted:** production in the Arctic will be limited by nitrogen availability and the extent to which species will adapt to these conditions remains unknown and needs to be addressed. This study aims to contribute to the understanding of N<sub>2</sub> fixation dynamics and its implications for ecosystem productivity with the rapidly evolving Arctic Ocean.<sup>1</sup>

We explored the diazotroph diversity in combination with N<sub>2</sub> fixation rate measurements, to elucidate the importance of this process in the Arctic ecosystem. We hope that understanding the dynamics of N<sub>2</sub> fixation and its impact on the ecosystem productivity can inform predictions and help managing the consequences of ongoing environme... [1]

**Deleted:** -

198 particulate organic carbon (POC) and nitrogen (PON), molecular samples for nucleic acid  
199 extractions (DNA), dissolved inorganic carbon (DIC) as well as CTD sensor data. At three selected  
200 stations (3,7,10) N<sub>2</sub> fixation and primary production rates were quantified through concurrent  
201 incubation experiments.

202 Samples for nutrient analysis, nitrate (NO<sub>3</sub><sup>-</sup>), nitrite (NO<sub>2</sub><sup>-</sup>) and phosphate (PO<sub>4</sub><sup>3-</sup>) were taken in  
203 triplicates, filtered through a 0.22  $\mu$ m syringe filter (Avantor VWR® Radnor, Pa, USA) and stored  
204 at -20 °C until further analysis. Concentrations were spectrophotometrically determined (Thermo  
205 Scientific, Genesys 1OS UV-VIS spectrophotometer) following the established protocols of  
206 Murphy and Riley (1962) for PO<sub>4</sub><sup>3-</sup>; García-Robledo et al. (2014) for NO<sub>3</sub><sup>-</sup> & NO<sub>2</sub><sup>-</sup> (detection  
207 limits: 0.01  $\mu$ mol L<sup>-1</sup> (NO<sub>3</sub><sup>-</sup>, NO<sub>2</sub><sup>-</sup>, and PO<sub>4</sub><sup>3-</sup>), 0.05  $\mu$ mol L<sup>-1</sup> (NH<sub>4</sub><sup>+</sup>)). Chl *a* samples were filtered  
208 onto 47 mm  $\phi$  GF/F filters (GE Healthcare Life Sciences, Whatman, USA), placed into darkened  
209 15 mL LightSafe centrifuge tubes (Merck, Rahway, NJ, USA) and were subsequently stored at -  
210 20 °C until further analysis. To determine the Chl *a* concentration, the samples were immersed in  
211 8 mL of 90 % acetone overnight at 5 °C. Subsequently, 1 mL of the resulting solution was  
212 transferred to a 1.5 mL glass vial (Mikrolab Aarhus A/S, Aarhus, Denmark) the following day and  
213 subjected to analysis using the Trilogy® Fluorometer (Model #7200-00) equipped with a Chl *a*  
214 in vivo blue module (Model #7200-043, both Turner Designs, San Jose, CA, USA). Measurements  
215 of serial dilutions from a 4 mg L<sup>-1</sup> stock standard and 90 % acetone (serving as blank) were  
216 performed to calibrate the instrument. In addition, measurements of a solid-state secondary  
217 standard were performed every 10 samples. Water (1 L) from each depth was filtered for the  
218 determination of POC and PON concentrations, as well as natural isotope abundance ( $\delta$  <sup>13</sup>C POC  
219 /  $\delta$  <sup>15</sup>N PON) using 47 mm  $\phi$ , 0.7  $\mu$ m nominal pore size precombusted GF/F filter (GE Healthcare  
220 Life Sciences, Whatman, USA), which were subsequently stored at -20 °C until further analysis.  
221 Seawater samples for DNA were filtered through 47 mm  $\phi$ , 0.22  $\mu$ m MCE membrane filter (Merck,  
222 Millipore Ltd., Ireland) for a maximum of 20 minutes, employing a gentle vacuum (200 mbar).  
223 The filtered volumes varied depending  
224 on the amount of material captured on the filter, ranging from 1.3 L to 2 L, with precise  
225 measurements recorded. The filters were promptly stored at -20 °C on the ship and moved to -80  
226 °C upon arrival to the lab until further analysis.  
227 To achieve detailed vertical profiles, a conductivity-temperature-depth-profiler (CTD, Seabird X)  
228 equipped with supplementary sensors for dissolved oxygen (DO), photosynthetic active radiation  
229 (PAR), and fluorescence (Fluorometer) was manually deployed.

## 230 2.2 Nitrogen fixation and primary production

231

**Formatted:** Superscript

**Formatted:** Subscript

**Formatted:** Superscript

**Formatted:** Subscript

**Formatted:** Superscript

**Formatted:** Subscript

**Formatted:** Superscript

**Formatted:** Superscript

**Deleted:** -

**Deleted:** -

**Deleted:**

**Deleted:** Seawater (40 ml) was filtered through a 0.22  $\mu$ m syringe filter (Avantor VWR® Radnor, Pa, USA) and stored at 4 °C in an amber glass vial, sealed with closed caps, affixed with a PTFE-faced silicon liner (Thermo Fisher Scientific, Waltham, MA, USA) for subsequent DIC measurements in the laboratory using an AS-C5 DIC analyzer (ApolloSciTech, Newark, Delaware, USA) equipped with a laser-based CO<sub>2</sub> detector. Sample analysis was carried out following the manufacturer's guidelines and the use of a certified seawater reference (Batch 187, Scripps Institution of Oceanography, University of California, San Diego, USA).

**Deleted:** In the same manner, discrete water samples were obtained using a 10 L Niskin bottle, manually lowered with a hand winch to five distinct depths (Surface, 5, 25, 50, 100 m). These systematic and multifaceted sampling methodologies provide a robust dataset for a comprehensive analysis of the hydrographic conditions in Qeqertarsuaq.

254 Water samples were collected at three distinct depths (0, 25 and 50 m) for the investigation of N<sub>2</sub>  
255 fixation rates and primary production rates, encompassing the euphotic zone, chlorophyll  
256 maximum, and a light-absent zone. Three incubation stations (Fig. 2: station 3, 7, 10) were chosen,  
257 in a way to cover the variability of the study area. This strategic sampling aimed to capture a  
258 gradient of the water column with varying environmental conditions, relevant to the aim of the  
259 study. N<sub>2</sub> fixation rates were assessed through triplicate incubations employing the modified <sup>15</sup>N-  
260 N<sub>2</sub> dissolution technique after Großkopf et al. (2012) and Mohr et al. (2010).

261 To ensure minimal contamination, 2.3 L glass bottles (Schott-Duran, Wertheim, Germany)  
262 underwent pre-cleaning and acid washing before being filled with seawater samples. Oxygen  
263 contamination during sample collection was mitigated by gently and bubble-free filling the bottles  
264 from the bottom, allowing the water to overflow. Each incubation bottle received a 100 mL  
265 amendment of <sup>15</sup>N-N<sub>2</sub> enriched seawater (98 %, Cambridge Isotope Laboratories, Inc., USA)  
266 achieving an average dissolved N<sub>2</sub> isotope abundance (<sup>15</sup>N atom %) of 3.90 ± 0.02 atom % (mean  
267 ± SD). Additionally, 1 mL of H<sup>3</sup>CO<sub>3</sub> (1g/50 mL) (Sigma- Aldrich, Saint Louis Missouri US) was  
268 added to each incubation bottle, roughly corresponding to 10 atom % enrichment and thus  
269 measurements of primary production and N<sub>2</sub> fixation were conducted in the same bottle. Following  
270 the addition of both isotopic components, the bottles were closed airtight with septa-fitted caps and  
271 incubated for 24 hours on-deck incubators with a continuous surface seawater flow. These  
272 incubators, partially shaded (using daylight-filtering foil) to simulate in situ photosynthetically  
273 active radiation (PAR) conditions, aimed to replicate environmental parameters experienced at the  
274 sampled depths. Control incubations utilizing atmospheric air served as controls to monitor any  
275 natural changes in  $\delta$  <sup>15</sup>N not attributable to <sup>15</sup>N-N<sub>2</sub> addition. These control incubations were  
276 conducted using the dissolution method, like the <sup>15</sup>N-N<sub>2</sub> enrichment experiments, but with the  
277 substitution of atmospheric air instead of isotopic tracer.

278 After the incubation period, subsamples for nutrient analysis were taken from each incubation  
279 sample, and the remaining content was subjected to the filtration process and were gently filtered  
280 (200 mbar) onto precombusted GF/F filters (Advantec,  
281 47 mm ø, 0.7  $\mu$ m nominal pore size). This step ensured a comprehensive examination of both  
282 nutrient dynamics and the isotopic composition of the particulate pool in the incubated samples.  
283 Samples were stored at -20 °C until further analysis.

284 Upon arrival in the lab, the filters were dried at 60 °C and to eliminate particulate inorganic carbon,  
285 subsequently subject to acid fuming during which they were exposed to concentrated hydrochloric  
286 acid (HCL) vapors overnight in a desiccator. After undergoing acid treatment, the filters were  
287 carefully dried, then placed into tin capsules and pelletized for subsequent analysis. The

← Formatted: Indent: Left: 0,15 cm, Right: 0,36 cm, Space  
Before: 0,7 pt

288 determination of POC and PON, as well as isotopic composition ( $\delta^{13}\text{C}$  POC /  $\delta^{15}\text{N}$  PON), was  
289 carried out using an elemental analyzer (Flash EA, ThermoFisher, USA) connected to a mass  
290 spectrometer (Delta V Advantage Isotope Ratio MS, ThermoFisher, USA) with the ConFlo IV  
291 interface. This analytical setup was applied to all filters. These values, derived from triplicate  
292 incubation measurements, exhibited no omission of data points or identification of outliers. Final rate  
293 calculations for  $\text{N}_2$  fixation rates were performed after Mohr et al. (2010) and primary production  
294 rates after Slawyk et al. (1977). [A detailed sensitivity analysis of  \$\text{N}\_2\$  fixation rates, including the  
contribution of each source of error for all parameters, is provided in a supplementary table and  
summarized form in the Appendix \(Table A1\).](#)

297 **2.3 Molecular methods**

298 The filters were flash-frozen in liquid nitrogen, crushed and DNA was extracted using the Qiagen  
299 DNA/RNA AllPrep Kit (Qi- agen, Hildesheim, DE), following the procedure outlined by the  
300 manufacturer. The concentration and quality of the extracted DNA was assessed  
301 spectrophotometrically using a MySpec spectrophotometer (VWR, Darmstadt, Germany). The  
302 prepara- tion of the metagenome library and sequencing were performed by BGI (China).  
303 Sequencing libraries were generated using MGIEasy Fast FS DNA Library Prep Set following the  
304 manufacturer's protocol. Sequencing was conducted with 2x150bp on a DNBSEQ-G400 platform  
305 (MGI). SOAPnuke1.5.5 (Chen et al. (2018)) was used to filter and trim low quality reads and  
306 adaptor contaminants from the raw sequence reads, as clean reads. In total, fifteen metagenomic  
307 datasets were produced with an average of 9.6G bp per sample.

309 **2.3.1 Metagenomic De Novo assembly, gene prediction, and annotation**

310 Megahit v1.2.9 [\(Li et al. \(2015\)\)](#) was used to assemble clean reads for each dataset with its  
311 minimum contig length as 500. Prodigal v2.6.3 (Hyatt et al. (2010)) with the setting of “-p meta”  
312 was then used to predict the open reading frames (ORFs) of the assembled contigs. ORFs from all  
313 the available datasets were filtered (>100bp), dereplicated and merged into a catalog of non-  
314 redundant genes using cd-hit-est (>95 % sequence identity) (Fu et al. (2012)). Salmon v1.10.0  
315 (Patro et al. (2017)) with the “– meta” option was employed to map clean reads of each dataset to  
316 the catalog of non-redundant genes and generate the GPM (genes per million reads) abundance.  
317 Eggnog mapper v2.1.12 (Cantalapiedra et al. (2021)) was then performed to assign KEGG  
318 Orthology (KO) and identify specific functional annotation for the catalog of non-redundant genes.  
319 The marker genes, *nifDK* (K02586, K02591 nitrogenase molybdenum-iron protein alpha/beta  
320 chain) [and](#) *nifH* (K02588, nitrogenase iron protein), were used for the evaluation of microbial

Formatted: Indent: Left: 0,14 cm, Right: 0,66 cm, Space Before: 0,05 pt

Field Code Changed

Field Code Changed

Deleted: ,

323 potential of N<sub>2</sub> fixation. *RbcL* (K01601, ribulose-bisphosphate carboxylase large chain) and *psbA*  
324 (K02703, photosystem II P680 reaction center D1 protein) were selected to evaluate the microbial  
325 potential of carbon fixation and photosynthesis, respectively. [The molecular datasets have been](#)  
326 [deposited with the accession number: Bioproject PRJNA1133027.](#)

Deleted: ¶

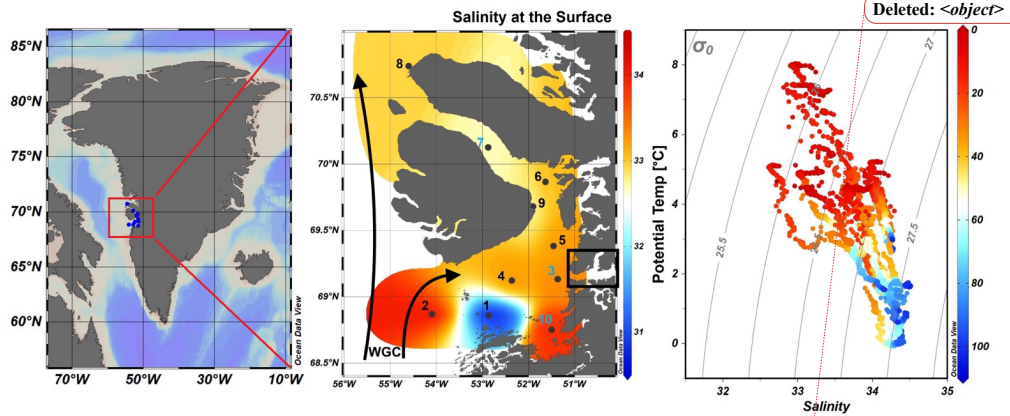
Formatted: Font: 10 pt

### 327 3 Results and discussion

#### 328 3.1 Hydrographic conditions in Qeqertarsuaq (Disco Bay) and Sullorsuaq (Vaigat) Strait

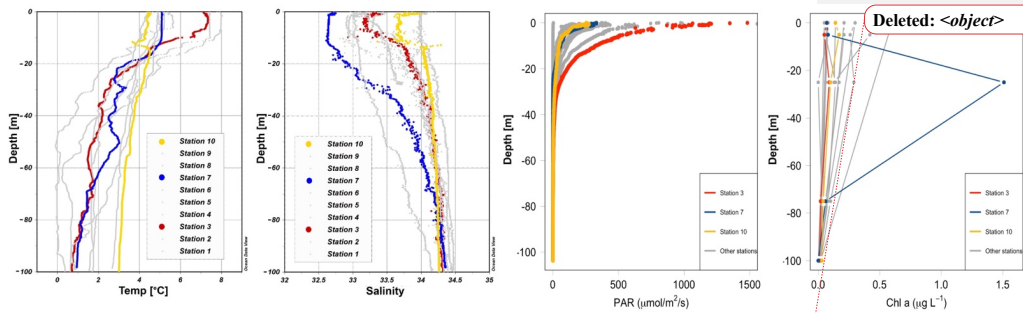
329 Disko Bay (Qeqertarsuaq) is located along the west coast of Greenland (Kalaallit Nunaat) at  
330 approximately 69 °N (Figure 1), and is strongly influenced by the West Greenland Current (WGC)  
331 which is associated with the broader Baffin Bay Polar Waters (BBPW) (Mortensen et al., 2022;  
332 Hansen et al., 2012). The WGC does not only significantly shape the hydrographic conditions  
333 within the bay but also plays an important role in the larger context of Greenland Ice Sheet melting  
334 (Mortensen et al. (2022)). Central to the hydrographic system of the Qeqertarsuaq area is the  
335 Jakobshavn Isbræ, which is the most productive glacier in the northern hemisphere and believed  
336 to drain about 7 % of the Greenland Ice Sheet and thus contributes substantially to the water influx  
337 into the Qeqertarsuaq (Holland et al. (2008)). A predicted increased inflow of warm subsurface  
338 water, originating from North Atlantic waters, has been suggested to further affect the melting of  
339 the Jakobshavn Isbræ and thus adds another layer of complexity to this dynamic system (Holland  
340 et al., 2008; Hansen et al., 2012).

341 The hydrographic conditions in Qeqertarsuaq have a significant influence on biological processes,  
342 nutrient availability, and the



348 **Figure 1.** Map of Greenland (Kalaallit Nunaat) with indication of study area (red box), on the left.  
 349 Interpolated distribution of Sea Surface Salinity (SSS) values with corresponding isosurface lines and  
 350 indication of 10 sampled stations (normal stations in black, incubation stations in blue), black arrows indicate  
 351 the West Greenland Current (WGC) and the black box indicate the location of the Jakobshavn Isbrae, in  
 352 the middle. Scatterplot of the potential temperature and salinity for all station data. The plot is used for the  
 353 identification of the main water masses within the study area. Isopycnals ( $\text{kg m}^{-3}$ ) are depicted in grey lines,  
 354 on the right. Figures were created in Ocean Data View (ODV) (Schlitzer (2022)).

355 broader marine ecosystem (Munk et al., 2015; Hendry et al., 2019; Schiøtt, 2023).  
 356 During our survey, we found very heterogeneous hydrographic conditions at the different stations  
 357 across Qeqertarsuaq (Fig. 1 & Fig. 2). The three selected stations for  $\text{N}_2$  fixation analysis (stations  
 358 3, 7, and 10) were strategically chosen to capture the spatial  
 359 variability of the area. Surface salinity and temperature measurements at these stations indicate  
 360 the influence of freshwater input. The surface temperature exhibit a range of 4.5 to 8 °C, while  
 361 surface salinity varies between 31 and 34, as illustrated in Fig. 1. The profiles sampled during  
 362 our survey extend to a maximum depth of 100 m. Comparison of temperature/salinity (T/S) plots  
 363 with recent studies suggests the presence of previously described water masses, including Warm  
 364 Fjord Water (WFjW) and Cold Fjord Water (CFjW) with an overlaying surface glacial meltwater  
 365 runoff. Those water masses are defined with a density range of  $27.20 \leq \sigma_0 \leq 27.31$  but different  
 366 temperature profiles. Thus water masses can be differentiated by their temperature within the same  
 367 density range (Gladish et al. (2015)). Other water masses like upper subpolar mode water  
 368 (uSPMW), deep subpolar mode water (dSPMW) and Baffin Bay polar Water (BBPW) which has  
 369 been identified in the Disko Bay (Qeqertarsuaq) before, cannot be identified from this data and  
 370 may be present in deeper layers (Mortensen et al., 2022; Sherwood et al., 2021; Myers and  
 371 Ribegaard, 2013; Rysgaard et al., 2020). The temperature and salinity profiles across the 10  
 372



Deleted: conservative

Deleted: <object>

376

377

378 **Figure 2.** Profiles of temperature (°C), salinity, photosynthetically active radiation (PAR) (μmol/m<sup>2</sup>/s) and  
379 Chl *a* (mg m<sup>-3</sup>) across stations 1 to 10 with depth (m). Stations 3, 7, and 10 are highlighted in red, blue, and  
380 yellow, respectively, to emphasize incubation stations. Figures were created in Ocean Data View and R-  
381 Studio (Schlitzer (2022)).

382

383 stations in the study area show distinct stratification and variability, which is represented through  
384 the three incubation stations (highlighted stations 3, 7, and 10 in Fig. 2). They display varying  
385 degrees of stratification and mixing, with notable differences in the salinity and temperature  
386 profiles. Station 3 and station 7 exhibit clear stratification in both temperature and salinity marked  
387 by the presence of thermoclines and haloclines. These features suggest significant freshwater input  
388 influenced by local weather conditions and climate dynamics, like surface heat absorption. In  
389 contrast, Station 10 exhibits a narrower range of temperature and salinity values throughout the  
390 water column compared to Stations 3 and 7, indicating more well-mixed conditions. This  
391 uniformity is likely influenced by the regional circulation pattern and partial upwelling (Hansen et  
392 al., 2012; Krawczyk et al., 2022). The distinct characteristics observed at station 10, as illustrated  
393 in the surface plot (Fig. 1), show an elevated salinity and colder temperatures compared

394

395 to the other stations. This feature suggests upwelling of deeper waters along the shallower shelf,  
396 likely facilitated by the local seafloor topography. Specifically, the seafloor shallowing off the coast  
397 of Station 10 may act as a barrier, disrupting typical circulation and forcing deeper, saltier, and  
398 colder waters to the surface. This pattern aligns with previous studies that describe similar  
399 mechanisms in the region (Krawczyk et al. (2022)). Their description of the bathymetry in  
400 Qeqertarsuaq, featuring depths ranging from ca. 50 to 900 m, suggests its impact on turbulent  
401 circulation patterns, leading to the mixing of different water masses. Evident variability in  
402 oceanographic conditions that can be observed throughout the study area occurs particularly along  
403 characteristic topographical features like steep slopes, canyons, and shallower areas. The summer  
404 melting of sea ice and glaciers introduces freshwater influxes that create distinct vertical and  
405 horizontal gradients in salinity and temperature in the Qeqertarsuaq area Hansen et al. (2012).  
406 Additionally, the accelerated melting of the Jakobshavn Isbraæ, influenced by the warmer inflow  
407 from the West Greenland Intermediate Current (WGIC), further alters the hydrographic conditions.  
408 Recent observations indicate significant warming and shoaling of the WGIC, potentially enabling  
409 it to overcome the sill separating the Ilulissat Fjord from the Qeqertarsuaq area (Hansen et al.,  
410 2012; Holland et al., 2008; Myers and Ribergaard, 2013). This shift intensifies glacier melting,  
411 driving substantial changes in the local ecological dynamics (Ardyna et al., 2014; Arrigo et al.,  
412 2008; Bhatia et al., 2013).

← Formatted: Indent: Left: 0,14 cm, Right: 0,66 cm

Deleted: In contrast station 10 shows more homogeneous salinity and temperature throughout the water column, indicative of well-mixed conditions.

Deleted: ¶

← Formatted: Indent: Left: 0 cm

Deleted: likely influenced by the seafloor shallowing off the coast of station 10, which acts as a barrier and disrupts typical circulation. The presence of water masses forced to the surface due to this topographical feature may explain the observed properties at station 10. Furthermore, the variability in temperature and salinity conditions between stations, particularly in relation to topography, aligns with the findings of

424    3.2 N<sub>2</sub> Fixation Rate Variability and Associated Environmental Conditions

425  
426    We quantified N<sub>2</sub> fixation rates within the waters of Qeqertarsuaq, spanning from the surface to a  
427    depth of 50 m (Table 1). The rates ranged from 0.16 to 2.71 nmol N L<sup>-1</sup> d<sup>-1</sup> with all rates  
428    surpassing the minimum quantifiably rate (Appendix Table 1). Our findings represent rates at the  
429    upper range of those observed in the Arctic Ocean. Previous measurements in the region have  
430    been limited, with only one study in Baffin Bay by Blais et al. (2012), reporting rates of 0.02 nmol  
431    N L<sup>-1</sup> d<sup>-1</sup>, which are 1-2 orders of magnitude lower than our observations. Moreover, Sipler et al.  
432    (2017), reported rated in the coastal Chukchi Sea, with average values of 7.7 nmol N L<sup>-1</sup> d<sup>-1</sup>. These  
433    values currently represent some of the highest rates measured in Arctic shelf environments.  
434    Compared to these, our highest measured rate (2.71 nmol N L<sup>-1</sup> d<sup>-1</sup>) is lower, but still important,  
435    particularly considering the more Atlantic-influenced location of our study site. Sipler et al. (2017)  
436    also noted that a significant fraction of diazotrophs were <3 µm in size, suggesting that small  
437    unicellular diazotrophs play a dominant role in Arctic nitrogen fixation. Altogether, our data  
438    contribute to the growing evidence that N<sub>2</sub> fixation is a widespread and potentially significant  
439    nitrogen source across various Arctic regions. Simultaneous primary production rate  
440    measurements ranged from 0.07 to 3.79 µmol N L<sup>-1</sup> d<sup>-1</sup>, with the highest rates observed at station 7  
441    and generally higher values in the surface layers. Employing Redfield stoichiometry, the measured  
442    N<sub>2</sub> fixation rates accounted for 0.47 to 2.6 % (averaging 1.57 %) of primary production at our  
443    stations. The modest contribution to primary production suggests that N<sub>2</sub> fixation does not exert a  
444    substantial influence on the productivity of these waters during the time of the sampling. Rather,  
445    our N<sub>2</sub> fixation rates suggest primary production to depend mostly on additional nitrogen sources  
446    including regenerated, meltwater or land-based sources.

447    While the N:P ratio is commonly used to assess nutrient limitations relative to Redfield  
448    stoichiometry, most DIN and DIP measurements in our study were below detection limit (BDL),  
449    preventing a reliable calculation for this ratio. As such, we refrain from drawing conclusions based  
450    on N:P stoichiometry. Nevertheless, previous studies by Jensen et al. (1999) and Tremblay and  
451    Gagnon (2009), have identified nitrogen limitation in this region. Such biogeochemical conditions,  
452    when present, would be expected to generate a niche for N<sub>2</sub> fixing organisms (Sohm et al. (2011)).  
453    While N<sub>2</sub> fixation did not chiefly sustain primary production during our sampling campaign, we  
454    hypothesize that N<sub>2</sub> fixation has the potential to play a role in bloom dynamics under certain  
455    conditions. As nitrogen availability decreases  
456    during a bloom, it may provide a niche for N<sub>2</sub> fixation, potentially helping to extend the productive  
457    period of the bloom (Reeder et al. (2021)). Satellite data indicates that a fall bloom began in  
458    early August, following the annual spring bloom, as described by Ardyna et al. (2014). This double

Deleted: Elevated N<sub>2</sub> fixation rates might play a role in nutrient dynamics and bloom development

Deleted: Space Before: 0,05 pt, Line spacing: Multiple 1,44 li

Deleted: detection

Deleted: limit

Deleted: Compared to other European Arctic waters, our rates at the surface and at 25 m water depth fall within the reported range for Arctic estuarine stations (1.04 to 1.87 nmol N L<sup>-1</sup> d<sup>-1</sup>, (SD ± 0.76 to 1.19) and marine stations (0.11 to 0.12 nmol N L<sup>-1</sup> d<sup>-1</sup>, (SD ± 0.09 to 0.09) (Blais et al. (2012)). However, we observed some of the highest rates reported so far, particularly at the surface.

Deleted: relatively

Deleted: may

Deleted:

Formatted: Right: 0,66 cm, Space Before: 0,1 pt

Deleted: The N:P ratio, calculated as DIN to DIP, indicates a deficit in N for primary production based on Redfield stoichiometry (Fig. 3).

Deleted: The N:P ratio, calculated as DIN to DIP, indicates a deficit in N for primary production based on Redfield stoichiometry (Fig. 3). This aligns with findings presented

Deleted: who observed a similar

Deleted: -

Deleted: -

Deleted: the relatively high

Deleted: rates observed

Deleted: may

Deleted: ¶

Deleted: ing

489 bloom situation may be driven by increased melting and the subsequent input of bioavailable  
490 nutrients and iron (Fe) from meltwater runoff (Arrigo et al., 2017; Hopwood et al., 2016; Bhatia et  
491 al., 2013). The meltwater from the Greenland Ice Sheet is a significant source of Fe (Bhatia et  
492 al., 2013; Hawkings et al., 2015, 2014), which is a limiting factor especially for diazotrophs (Sohm et  
493 al. (2011)). Consequently, it is plausible that Fe and nutrients from the Isbrae glacier create  
494 favorable conditions for both bloom development and diazotroph activity in Qeqertarsuaq.  
495 However, we emphasize that confirming a causal link between N<sub>2</sub> fixation and secondary bloom  
496 development requires further evidence, such as time-series data on nutrient concentrations,  
497 diazotroph abundance, and bloom dynamics.

**Table 1.**  $\text{N}_2$  fixation (nmol N L<sup>-1</sup> d<sup>-1</sup>), standard deviation (SD), primary productivity (PP;  $\mu\text{mol C L}^{-1} \text{d}^{-1}$ ), SD, percentage of estimated new primary productivity (% New PP) sustained by  $\text{N}_2$  fixation, dissolved inorganic nitrogen compounds (NO<sub>x</sub>), phosphorus (PO<sub>4</sub>), and the molar nitrogen-to-phosphorus ratio (N:P) at stations 3, 7, and 10. BDL= Below detection limit.

Station (no.)	Depth (m)	N <sub>2</sub> fixation (nmol N L <sup>-1</sup> d <sup>-1</sup> )	SD (±)	Primary Productivity (μmol C L <sup>-1</sup> d <sup>-1</sup> )	SD (±)	% New PP (%)	NO <sub>x</sub> (μmol L <sup>-1</sup> d <sup>-1</sup> )	PO <sub>4</sub> (μmol L <sup>-1</sup> d <sup>-1</sup> )
3	0	1.20	0.21	0.466	0.08	1.71	BDL	0
3	25	1.88	0.11	0.588	0.04	2.11	BDL	0
3	50	0.29	0.01	0.209	0.00	0.91	0.33	1
7	0	2.49	0.44	0.63	0.20	2.60	BDL	0
7	25	2.71	0.22	3.79	2.45	0.47	BDL	0
7	50	0.53	0.24	0.33	0.36	1.08	BDL	0
10	0	1.48	0.12	0.74	0.15	1.33	BDL	0
10	25	0.31	0.01	0.29	0.07	0.73	BDL	0
10	50	0.16	0	0.07	0.07	1.40	BDL	0

504 A near-Redfield stoichiometry in POC:PON suggests, that the particulate organic matter (POM)  
505 likely originates, from an ongoing phytoplankton bloom, as phytoplankton generally assimilate  
506 carbon and nitrogen in relatively consistent proportions during active growth (Redfield 1934).  
507 However this assumption is based on a global average, and POM stoichiometry can exhibit  
508 substantial latitudinal variation. Deviations may also arise during particle production and  
509 remineralization processes (Redfield 1934; Geider and La Roche 2002; Sterner and Elser 2017;  
510 Quigg et al., 2003). Recent studies have further shown that POM composition vary widely across

**Deleted:** Consequently, it is possible that nutrients and Fe from the Isbrae glacier introduced into the Qeqertarsuaq are promoting a bloom and further provide a niche for diazotrophs to thrive (Arrigo et al. (2017)).

### Deleted: compounds

- Deleted:** 0
- Deleted:** 3 indicates
- Formatted:** Indent: Left: 0 cm, Line spacing: Multiple 1,46  
li
- Deleted:** is freshly derived

532 plankton communities, influenced by factors such as growth rates, community composition, ad  
533 physiological status (e.g. fast- vs- slow-growing organisms), with degradation often playing a  
534 secondary role (Tanioka et al., 2022). Additionally, terrestrial organic material—likely introduced  
535 via glacial outflow in the study area—may also contribute to the observed POM composition  
536 (Schneider et al., 2003). Latitudinal variability in organic matter stoichiometry has also been linked  
537 to differences in nutrient supply and phosphorus stress (Fagan et al., 2024; Tanioka et al., 2022).  
538 Consequently, the near-Redfield stoichiometry observed here cannot be clearly attributed to freshly  
539 produced organic material. Nevertheless, satellite-derived surface chlorophyll *a* concentration and  
540 associated primary production support the interpretation that recently produced organic matter does  
541 contribute, at least in part, to the sinking POM captured in our samples. Since inorganic nitrogen  
542 species (e.g., NO<sub>x</sub>) were below detection limits, direct calculation or interpretation of the N:P ratio  
543 in the dissolved nutrient pool was not possible and has been avoided. The absence of available  
544 nitrogen may nonetheless reflect nitrogen depletion, potentially creating ecological niches for  
545 diazotrophs and nitrogen-fixing organisms. Such conditions may promote shifts in microbial  
546 community structure, as observed by Laso-Perez et al. (2024). ▶▶ Laso Perez et al. (2024)  
547 documented changes in microbial community composition during an Arctic bloom, focusing on  
548 nitrogen cycling. They observed a shift from chemolithotrophic to heterotrophic organisms  
549 throughout the summer bloom and noted increased activity to compete for various nitrogen sources.  
550 However, no *nifH* gene copies, indicative of nitrogen-fixing organisms, were found in their dataset  
551 based on metagenome-assembled genomes (MAGs). This is not unexpected due to the classically  
552 low abundance of diazotrophs in marine microbial communities which has often been described  
553 (Turk-Kubo et al., 2015; Farnelid et al., 2019). Given the high productivity and metabolic activity  
554 observed in Qeqertarsuaq during a similar bloom period, the detected diazotrophs (Section 3.3)  
555 may play a more significant role than previously thought. Across the 10 stations there is  
556 considerable variability in POC and PON concentrations (Fig. 3). PON concentrations range from  
557 0.0  $\mu\text{mol N L}^{-1}$  to 3.48  $\mu\text{mol N L}^{-1}$  (n=124), while POC concentrations range from 2.7  $\mu\text{mol C L}^{-1}$   
558 to 27.2  $\mu\text{mol C L}^{-1}$  (n=144). The highest concentrations for both PON and POC were observed at  
559 station 7 at a depth of 25 m and coincide with the highest reported N<sub>2</sub> fixation rate (Figure Appendix  
560 A2 & A3). Generally, POC and PON concentrations decrease with depth, peaking at the deep chl  
561 *a* maximum (DCM), identified between 15 to 30 m across all stations. The DCM was identified  
562 based on measured chl *a* concentrations and previous descriptions in the region (Fox and Walker,  
563 2022; Jensen et al., 1999). The variability in chl *a* concentrations indicates differences in  
564 phytoplankton abundance among the stations, with concentrations ranging between 0 to 0.42 mg m<sup>-3</sup>.  
565 Excluding station 7, which exhibited the highest chl *a* concentration at the DCM (1.51 mg m<sup>-3</sup>).

**Deleted:** In contrast, deviations from the Redfield ratio (e.g., elevated C:N or C:P) typically indicate microbial degradation and preferential remineralization of nitrogen and phosphorus (Redfield 1934; Geider and La Roche 2002; Sterner and Elser 2017).

**Formatted:** Font: Italic

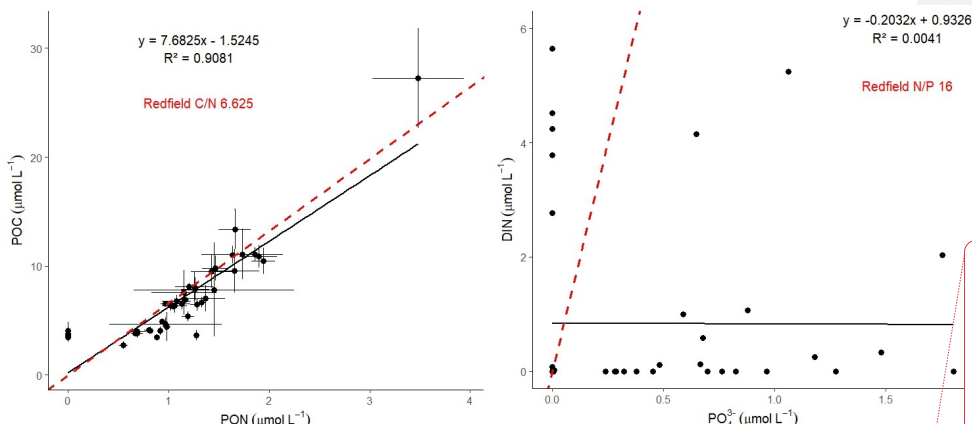
**Deleted:** bloom. However, the absence of NO<sub>x</sub> (with the exception of one station) and the observed low N:P ratios suggest that any available nitrogen from earlier phases of the bloom has likely been depleted. This could create a niche for N<sub>2</sub> fixation as a supplementary nitrogen source, potentially supporting continued production during this stage of the bloom. The onset and development of the bloom would be expected to lead to high nitrogen demands and intense competition for nitrogen sources. Notably, despite the apparent balance in the POM pool, the N ratio indicates strong nitrogen depletion and nutrient exhaustion within the ecosystem. This deficiency can be partly alleviated by N<sub>2</sub> fixation, providing possibly increasing amounts of nitrogen over the course of the bloom. Moreover, DIP is generally limited in the environment (Table 1); however, some organisms may still access it through luxury phosphorus uptake, storing excess phosphate when it is sporadically available.

**Deleted:** A recent study<sup>1</sup>  
by

**Deleted:** <sup>1</sup>

592 While Tang et al. (2019) found that  $N_2$  fixation measurements strongly correlated to satellite  
 593 estimates of chl *a* concentrations, our results did not show a statistically significant correlation  
 594 between nitrogen fixation rates and chl *a* concentrations overall (Figures A2 & A3). However, as  
 595 noted, Station 7 at 25 m represents a unique case. The elevated concentration of chl *a* at this station  
 596 likely resulted from a local phytoplankton bloom induced by meltwater outflow from the Isbrae  
 597 glacier and sea ice melting, which may help explain the observed nitrogen fixation rates (Arrigo et  
 598 al., 2017; Wang et al., 2014). This study's findings are in agreement with prior reports of analogous  
 599 blooms occurring in the region (Fox and Walker, 2022; Jensen et al., 1999).

600



601  
 602 **Figure 3.** The POC/PON and DIN/DIP ratios at all 10 stations. The red line represents the Redfield ratios of  
 603 POC/PON (106:16) and DIN/DIP (16:1).

604

605

### 606 3.3 Potential Contribution of UCYN-A to Nitrogen Fixation During a Diatom Bloom: Insights 607 and Uncertainties

608

609 In our metagenomic analysis, we filtered the *nif H*, *nif D*, *nif K* genes, which code for the  
 610 nitrogenase enzyme responsible for catalyzing  $N_2$  fixation. We could identify sequences related to  
 611 UCYN-A, which dominated the sequence pool of diazotrophs, particularly in the upper water  
 612 masses (0 to 5 m) (Fig. 4). UCYN-A, a unicellular cyanobacterial symbiont, has a cosmopolitan  
 613 distribution and is thought to substantially contribute to global  $N_2$  fixation, as documented by

• **Deleted:** stations there is considerable variability in POC and PON concentrations (Fig. 3). PON concentrations range from  $0.5 \mu\text{mol N L}^{-1}$  to  $4.0 \mu\text{mol N L}^{-1}$  ( $n=124$ ), while POC concentrations range from  $2.5 \mu\text{mol C L}^{-1}$  to  $32.6 \mu\text{mol C L}^{-1}$  ( $n=144$ ). The highest concentrations for both PON and POC were observed at station 7 at a depth of 25 m and coincide with the highest reported  $N_2$  fixation rate (Figure Appendix A2 & A3). Generally, POC and PON concentrations decrease with depth, peaking at the deep chl *a* maximum (DCM), identified between 15 to 30 m across all stations. The variability in chl *a* concentrations indicates differences in phytoplankton abundance among the stations, with concentrations ranging between 0 to  $0.42 \text{ mg m}^{-3}$ . Excluding station 7, which exhibited the highest chl *a* concentration at the DCM ( $1.51 \text{ mg m}^{-3}$ ). Tang et al. (2019) have found that  $N_2$  fixation measurements strongly correlated to satellite estimates of chl *a* concentrations and thus may be an explanation for the presented  $N_2$  fixation rates. The elevated concentration of chl *a* likely result from a local phytoplankton bloom induced by meltwater outflow from the Isbrae glacier and sea ice melting (Arrigo et al., 2017; Wang et al., 2014). This can also be seen<sup>1</sup>

**Deleted:** from satellite images (Appendix A1). This study's findings are in agreement with prior reports of analogous blooms occurring in the region (Fox and Walker, 2022; Jensen et al., 1999).<sup>1</sup>  
 UCYN...

**Deleted:** -A might contribute to  $N_2$  fixation during a diatom bloom...

643 (Martínez-Pérez et al., 2016; Tang et al., 2019). This conclusion is based on our metagenomic  
644 analysis, in which we set a sequence identity threshold of 95% for both *nif* and photosystem genes.  
645 Notably, we only recovered sequences related to UCYN-A within our *nif* sequence pool,  
646 suggesting its predominance among detected diazotrophs. However, metagenomic approaches  
647 may underestimate overall diazotroph diversity, and we cannot fully exclude the presence of other,  
648 less abundant diazotrophs that may have been missed using this method. While UCYN-A was  
649 primarily detected in surface waters, we also observed relatively high *nifK* values at S3\_100m, an  
650 unusual finding given that UCYN-A is typically constrained to the euphotic zone. Previous studies  
651 have predominantly reported UCYN-A in surface waters; for instance Harding et al. (2018) and  
652 Shiozaki et al. (2017) detected UCYN-A exclusively in the upper layers of the Arctic Ocean.  
653 Additionally, Shiozaki et al. (2020) found UCYN-A2 at depths extending to the 0.1% light level  
654 but not below 66 m in the Chukchi Sea. The detection of UCYN-A at 100 m in our study suggests  
655 that alternative mechanisms, such as particle association, vertical transport, or local environmental  
656 conditions, may facilitate its presence at depth. Interestingly, despite very low *nifH* copy numbers  
657 being reported in nearby Baffin Bay by Robicheau et al. (2023), UCYN-A dominated the  
658 metagenomic *nifH* community in our study, further underscoring this organism's presence in  
659 Arctic surface coastal areas under certain environmental conditions. This warrants further  
660 investigation into the environmental drivers and potential processes enabling its occurrence in  
661 Arctic waters.

662 Due to the lack of genes such as those encoding Photosystem II and Rubisco, UCYN-A plays a  
663 significant role within the host cell and participates in fundamental cellular processes.  
664 Consequently, it has evolved to become a closely integrated component of the host cell. Very  
665 recent findings demonstrate that UCYN-A imports proteins encoded by the host genome and has  
666 been described as an early form of N<sub>2</sub> fixing organelle termed a "Nitroplast" (Coale et al. (2024)).  
667 Previous investigations document that they are critical for primary production, supplying up to 85%  
668 of the fixed nitrogen to their haptophyte host (Martínez-Pérez et al. (2016)). In addition to its high  
669 contribution to primary production, studies have shown that UCYN-A in high latitude waters fix  
670 similar amounts of N<sub>2</sub> per cell as in the tropical Atlantic Ocean, even in nitrogen- replete waters  
671 (Harding et al., 2018; Shiozaki et al., 2020; Martínez-Pérez et al., 2016; Krupke et al., 2015; Mills  
672 et al., 2020). However, estimating their contribution to N<sub>2</sub> fixation in our study is challenging,  
673 particularly since we detected cyanobacteria only at the surface but observe significant N<sub>2</sub> fixation  
674 rates below 5 m. The diazotrophic community is often underrepresented in metagenomic datasets  
675 due to the low abundance of nitrogenase gene copies, implying our data does, not present a  
676 complete picture. We suspect a more diverse diazotrophic community exists, with UCYN-A being

Formatted: Font: Italic

Deleted: Consequently

Deleted: may

679 a significant contributor to N<sub>2</sub> fixation in Arctic waters. However, the exact proportion of its  
680 contribution requires further investigation.

681 The contribution of N<sub>2</sub> fixation to carbon fixation (as percent of PP) is relatively low, at the time of  
682 our study. We identified genes such as *rbcL*, which encodes Rubisco, a key enzyme in the carbon  
683 fixation pathway and *psbA*, a gene encoding Photosystem II, involved in light-driven electron  
684 transfer in photosynthesis, in our metagenomic dataset. The gene *rbcL* (for the carbon fixation  
685 pathway) and the gene *psbA* (for primary producers) were used to track the community of  
686 photosynthetic primary producers in our metagenomic dataset. At station 7, elevated carbon  
687 fixation rates are correlated with high diatom (*Bacillariophyta*) abundance and increased chl *a*  
688 concentration (Fig. 4), suggesting the onset of a bloom, which is also observable via satellite images  
689 (Appendix A1). We hypothesize that meltwater, carrying elevated nutrient and trace metal  
690 concentrations, was rapidly transported away from the glacier through the Vaigat Strait by strong  
691 winds, leading to increased productivity, as previously described by Fox and Walker (2022) &  
692 Jensen et al. (1999). The elevated diatom abundance and primary production rates at station 7  
693 coincide with the highest N<sub>2</sub> fixation rates, which could point toward a possible diatom-diazotroph  
694 symbiosis (Foster et al., 2022, 2011; Schwarcz et al., 2022). However, we did not detect a clear  
695 diazotrophic signal directly associated with the diatoms in our metagenomic dataset, which might be  
696 due to generally underrepresentation of diazotrophs in metagenomes due to low abundance or  
697 low sequencing coverage. To investigate this further, we examined the taxonomic  
698 composition of *Bacillariophyta* at higher resolution. Among the various abundant diatom  
699 genera, *Rhizosolenia* and *Chaetoceros* have been identified as symbiosis with diazotrophs  
700 (Grosse, et al., 2010; Foster, et al., 2010), representing less than 6% or 15% of  
701 *Bacillariophyta*, based on *rbcL* or *psbA*, respectively (Figure Appendix A4). Although we  
702 underestimate diazotrophs to an extent, the presence of certain diatom-diazotroph symbiosis  
703 could help explain the high nitrogen fixation rates in the diatom bloom to a certain degree.  
704 Compilation of *nif* sequences identified from this study as well as homologous from their  
705 NCBI top hit were added in Table S1. However, we cannot tell if the diazotrophs belong to  
706 UCYN-A1 or UCYN-A2, or UCYN-A3. Based on the Pierella Karlusich et al. (2021), they  
707 generated clonal *nifH* sequences from Tara Oceans, which the length of *nifH* sequences is  
708 much shorter than the two *nifH* sequences we generated in our study. Also, the available  
709 UCYN-A2 or UCYN-A3 *nifH* sequences from NCBI were shorter than the two *nifH* sequences  
710 we generated. Therefore, it would be not accurate to assign the *nifH* sequences to either group  
711 under UCYN-A. Furthermore, not much information is available regarding the different  
712 groups of UCYN-A using marker genes of *nifD* and *nifK*.

713 ↶ Formatted: Indent: Left: 0 cm

Deleted: but may increase with a further onset of bloom periods.

Deleted: possibly

Deleted: s

Deleted: However,

Deleted: ny relevant

Deleted: group

Deleted: observed

Deleted: their absence or due to the

Deleted: .

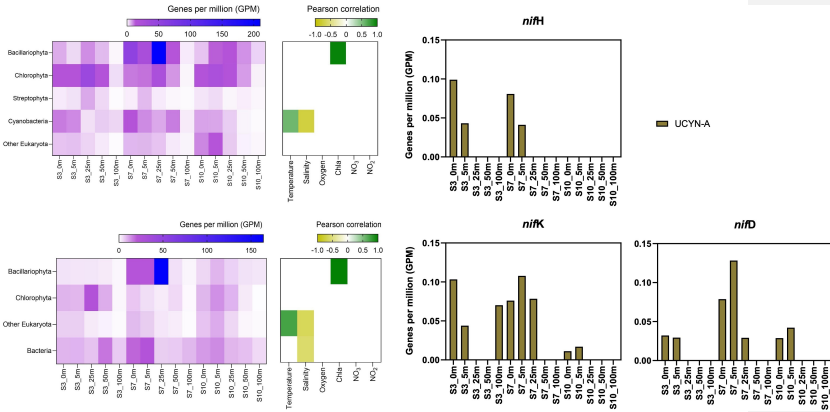
Formatted: Font: Italic

Moved (insertion) [1]

Deleted: Therefore, we can only assume that such a symbiosis explains the elevated rates. Additional molecular approaches would be necessary to enhance our understanding show a more detailed picture of the diazotrophic community.¶

Moved up [1]: a symbiosis explains the elevated rates. Additional molecular approaches would be necessary to enhance our understanding show a more detailed picture of the diazotrophic community.¶

Deleted: ¶



734  
 735 **Figure 4.** Upper left image: *psbA* with correlation plot. Lower left image: *rbcL* with correlation plot. Right  
 736 image: *nifH*, *nifD*, *nifK* genes per million reads in the metagenomic datasets. All figures display molecular  
 737 data from metagenomic dataset for all sampled depth of station 3,7,10

740  
 741 There is evidence that UCYN-A have a higher Fe demand, with input through meltwater or river  
 742 runoff potentially being advantageous to those organisms (Shiozaki et al., 2017, 2018; Cheung et  
 743 al., 2022). Consequently, UCYN-A might play a more critical role in the future with increased Fe-  
 744 rich meltwater runoff. UCYN-A can potentially fuel primary productivity by supplying nitrogen,  
 745 especially with increased melting, nutrient inputs, and more light availability due to rising  
 746 temperatures associated with climate change. This predicted enhancement of primary productivity  
 747 may contribute to the biological drawdown of CO<sub>2</sub>, acting as a negative feedback mechanism.  
 748 These projections are based on studies forecasting increased temperatures, melting, and resulting  
 749 biogeochemical changes leading to higher primary productivity. However large uncertainties make  
 750 predictions very difficult and should be handled with care. ~~Thus~~, we can only hypothesize that  
 751 UCYN-A might be coupled to these dynamics by providing essential nitrogen.

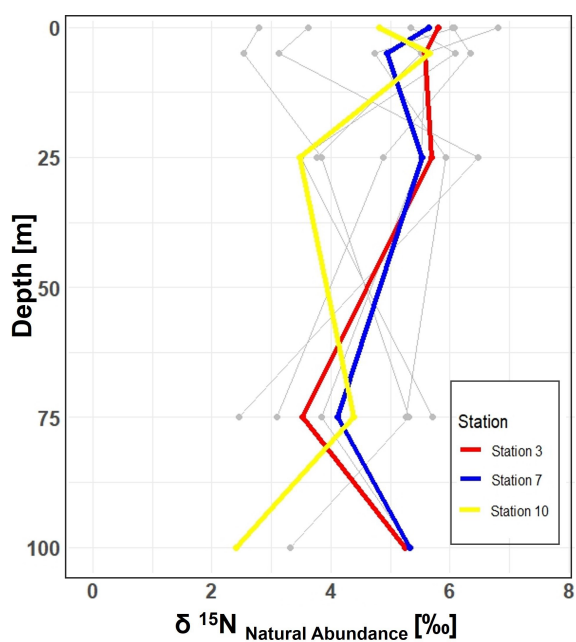
Deleted: Thus

Deleted: show no clear evidence of nitrogen fixation

### 752 3.4 $\delta^{15}\text{N}$ Signatures in particulate organic nitrogen

753 Stable isotopic composition, expressed using the  $\delta^{15}\text{N}$  notation, serve as indicators for  
 754 understanding nitrogen dynamics because different biogeochemical processes fractionate nitrogen  
 755 isotopes in distinct ways (Montoya (2008)). However, it is important to keep in mind that the final  
 756 isotopic signal is a combination of all processes and an accurate distinction between processes

760 cannot be made.  $\text{N}_2$  fixation tends to enrich nitrogenous compounds with lighter isotopes,  
761 producing OM with isotopic values ranging approximately from -2 to +2 ‰ (Dähnke and  
762 Thamdrup (2013)). Upon complete remineralization and oxidation, organic matter contributes to  
763 a reduction in the average  $\delta$ -values in the open ocean (e.g. Montoya et al. (2002);  
764 Emeis et al. (2010)). Whereas processes like denitrification and anammox preferentially remove  
765 lighter isotopes, leading to enrichment in heavier isotopes and delta values up to -25 ‰.  
766



767  
768 **Figure 5.** Vertical profiles of  $\delta^{15}\text{N}$  natural abundance signatures in PON across 10 stations in the study area.  
769 Incubation stations 3, 7, and 10 are highlighted in red, blue, and yellow, respectively. The figure shows  
770 variations in  $\delta^{15}\text{N}$  signatures with depth at each station, providing insight into nitrogen cycling in the study  
771 area.

772  
773 In our study, the  $\delta^{15}\text{N}$  values of PON from all 10 stations, range between 2.45 ‰ and 8.30 ‰  
774 within the 0 to 100 m depth range. While  $\text{N}_2$  fixation typically produces OM ranging from -2 ‰ to 0.5

**Deleted:** Thus,  $\delta^{15}\text{N}$  values help to identify different processes of the nitrogen cycle generally present in a system (Dähnke and Thamdrup (2013)).

779 ~~%, this signal can be masked by processes such as remineralization, mixing with nitrate from~~  
780 ~~deeper waters or other biological transformations (Emeis et al. (2010); Sigman et al. (2009)). The~~  
781 ~~composition of OM in the surface ocean is influenced by the nitrogen substrate and the~~  
782 ~~fractionation factor during assimilation. When nitrate is depleted in the surface ocean, the isotopic~~  
783 ~~signature of OM produced during photosynthesis will mirror that of the nitrogen source. Nitrate,~~  
784 ~~the primary form of dissolved nitrogen in the open ocean, typically exhibits an average stable~~  
785 ~~isotope value of around~~  
786 5 %. No fractionation occurs during photosynthesis because the nitrogen source is entirely taken  
787 up in the surface waters (Sigman et al. (2009)). ~~This matches conditions observed in Qeqertarsuaq,~~  
788 ~~suggesting that subsurface nitrate is a dominant nitrogen source (Fox and Walker (2022)).~~  
789 In the eastern Baffin Bay waters, Atlantic water masses serve as an important source of nitrate ~~to~~  
790 ~~surface waters with  $\delta^{15}\text{N}$  values around 5 %~~ (Sherwood et al. (2021)). ~~This is consistent with our~~  
791 ~~observed PON values and supports the view that primary productivity in the region is largely~~  
792 ~~fueled by nitrate input from deeper Atlantic waters, particularly during early bloom stages (Fox~~  
793 and Walker, 2022; Knies, 2022). The mechanisms through which subsurface nitrate reaches the  
794 euphotic layer are not well understood. However, potential pathways include vertical migration of  
795 phytoplankton and physical mixing. Subsequently, nitrogen undergoes rapid recycling and  
796 remineralization processes to meet the system's nitrogen demands (Jensen et al. (1999)). ~~Taken~~  
797 ~~together, the  $\delta^{15}\text{N}$  signatures observed in this study are best interpreted as indicative of a system~~  
798 ~~influenced by multiple nitrogen sources and biogeochemical processes, where nitrate input and~~  
799 ~~remineralization appear to dominate.~~

#### 801 4 Conclusion

802 Our study highlights the occurrence of elevated rates of  $\text{N}_2$  fixation in Arctic coastal waters,  
803 particularly prominent at station 7, where they coincide with high chl *a* values, indicative of  
804 heightened productivity. Satellite observations tracing the origin of a bloom near the Isbrae Glacier,  
805 subsequently moving through the Vaigat strait, suggest a recurring phenomenon likely triggered by  
806 increased nutrient-rich meltwater originating from the glacier. This aligns with previous reports  
807 by Jensen et al. (1999) & Fox and Walker (2022), underlining the significance of such events in  
808 driving primary productivity in the region. The contribution of  $\text{N}_2$  fixation to primary production  
809 was low (average 1.57 %) across the stations. Since the demand was high relative to the new  
810 nitrogen provided by  $\text{N}_2$  fixation, the observed primary production must be sustained by the already

811 **Deleted:** , thus do not exhibit a clear signal indicative of  $\text{N}_2$  fixation.

812 **Deleted:** This suggests that  $\text{N}_2$  fixation likely contributes only a certain fraction to export production or that it only started to contribute to isotope fractionation in the bloom dynamic.

813 **Deleted:** pho- tosynthesis

814 **Deleted:** substrate

815 **Deleted:** This substrate can originate from either nitrate in the subsurface or  $\text{N}_2$  fixation. Notably, n

816 **Deleted:** In

817 **Deleted:** where similar conditions prevail, this suggests that factors other than  $\text{N}_2$  fixation may be influencing the observed  $\delta$ -values and POM is sustained by nitrogen sources from deeper subsurface waters, as observed in earlier studies

818 **Deleted:** for sustaining primary productivity, which is also reflected in the nitrogen isotopic signature in this study

819 **Deleted:** The influx of Atlantic waters, characterized by  $\text{NO}_3^-$  values of approximately 5 %, closely matches the  $\delta^{15}\text{N}$  values of observed PON concentrations in our study. This suggests that Atlantic-derived  $\text{NO}_3^-$  serves as a primary source of new nitrogen to the initial stages of bloom development

820 **Deleted:** As the bloom progresses and nitrogen from Atlantic waters is depleted,  $\text{N}_2$  fixation may provide an additional nitrogen source, supporting continued primary productivity. ...

841 present or adequate amount of subsurface supply of  $\text{NO}_x$  nutrients in the seawater. This is also  
842 visible in the isotopic signature of the POM (Fox and Walker, 2022; Sherwood et al., 2021).  
843 However, the detected  $\text{N}_2$  fixation rates are likely linked to the development of the fresh secondary  
844 summer bloom, which could be sustained by high nutrient and Fe availability from melting,  
845 potentially leading the system into a nutrient-limited state. The ongoing high demand for nitrogen  
846 compounds may suggest an onset to further sustain the bloom, but it remains speculative whether  
847 Fe availability definitively contributes to this process. The occurrence of such double blooms has  
848 increased by 10 % in the Qeqertarsuaq and even 33 % in the Baffin Bay, with further projected  
849 increases moving north from Greenland (Kalaallit Nunaat) waters (Ardyna et al. (2014)). Thus,  
850 nutrient demands are likely to increase, and the role of  $\text{N}_2$  fixation ~~can~~ become more significant.  
851 The diazotrophic community in this study is dominated by UCYN-A in surface waters and may be  
852 linked to diatom abundance in deeper layers. This co-occurrence of diatoms and  $\text{N}_2$  fixers in the  
853 same location is probably due to the co-limitation of similar nutrients, rather than a symbiotic  
854 relationship. Thus, this highlights the significant presence of diazotrophs despite their limited  
855 representation in datasets. It also highlights the potential for further discoveries, as existing datasets  
856 likely underestimate the full extent of the diazotrophic community (Laso Perez et al., 2024;  
857 Shao et al., 2023; Shiozaki et al., 2017, 2023). The reported  $\text{N}_2$  fixation rates in the Vaigat strait  
858 within the Arctic Ocean are notably higher than those observed in many other oceanic regions,  
859 emphasizing that  $\text{N}_2$  fixation is an active and significant process in these high-latitude waters.  
860 When compared to measured rates across various ocean systems using the  $^{15}\text{N}$  approach, the  
861 significance of these findings becomes clear. For instance,  $\text{N}_2$  fixation rates are sometimes below  
862 the detection limit and often relatively low ranging from 0.8 to 4.4 nmol  $\text{N L}^{-1} \text{d}^{-1}$  (Löschner et al.,  
863 2020, 2016; Turk et al., 2011). In contrast, higher rates reach up to 20 nmol  $\text{N L}^{-1} \text{d}^{-1}$  (Rees et al.  
864 (2009)) and sometime exceptional high rates range from 38 to 610 nmol  $\text{N L}^{-1} \text{d}^{-1}$  (Bonnet et al.  
865 (2009)). The Arctic Ocean rates are thus significant in the global context, underscoring the  
866 region's role in the global nitrogen cycle and the importance of  $\text{N}_2$  fixation in supporting primary  
867 productivity in these waters.  
868 These findings highlight the urgent need to understand the interplay between seasonal variations,  
869 sea-ice dynamics, and hydro- graphic conditions in Qeqertarsuaq. As climate change accelerates  
870 the melting of the Greenland Ice Sheet at Jakobshavn Isbræ, shifts in hydrodynamic patterns and  
871 hydrographic conditions in Qeqertarsuaq are anticipated. The resulting influx of warmer waters  
872 could significantly reshape the bay's hydrography, making it crucial to comprehend the coupling  
873 of climate-driven changes and oceanic processes in this vital Arctic region. Our study provides key  
874 insights into these dynamics and underscores the importance of continued investigation to predict

Deleted: may

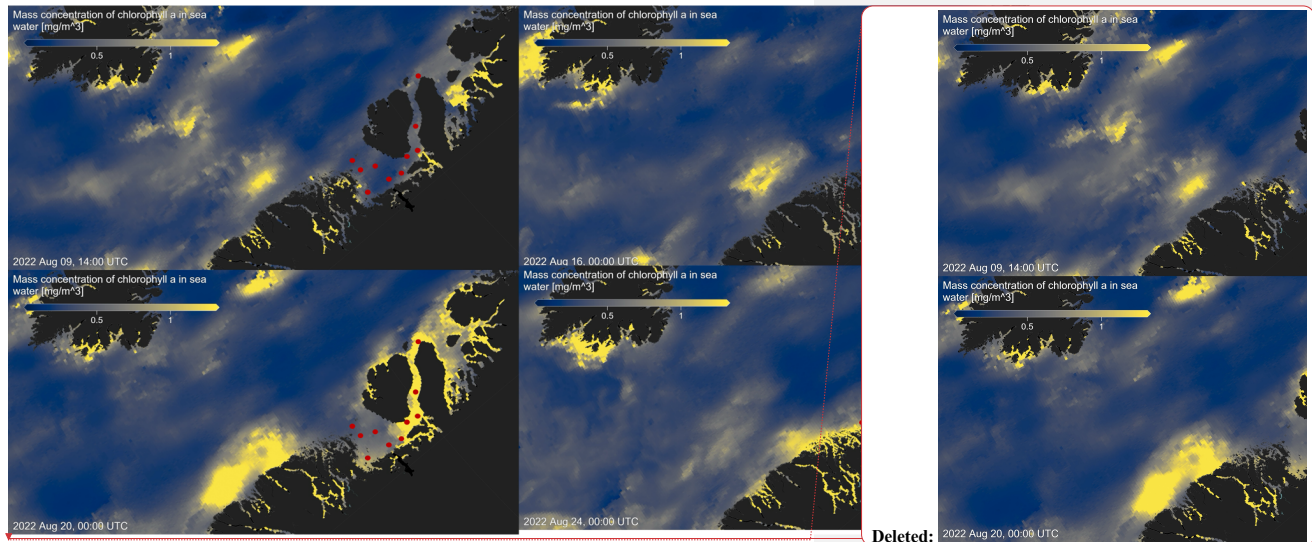
Field Code Changed  
Field Code Changed

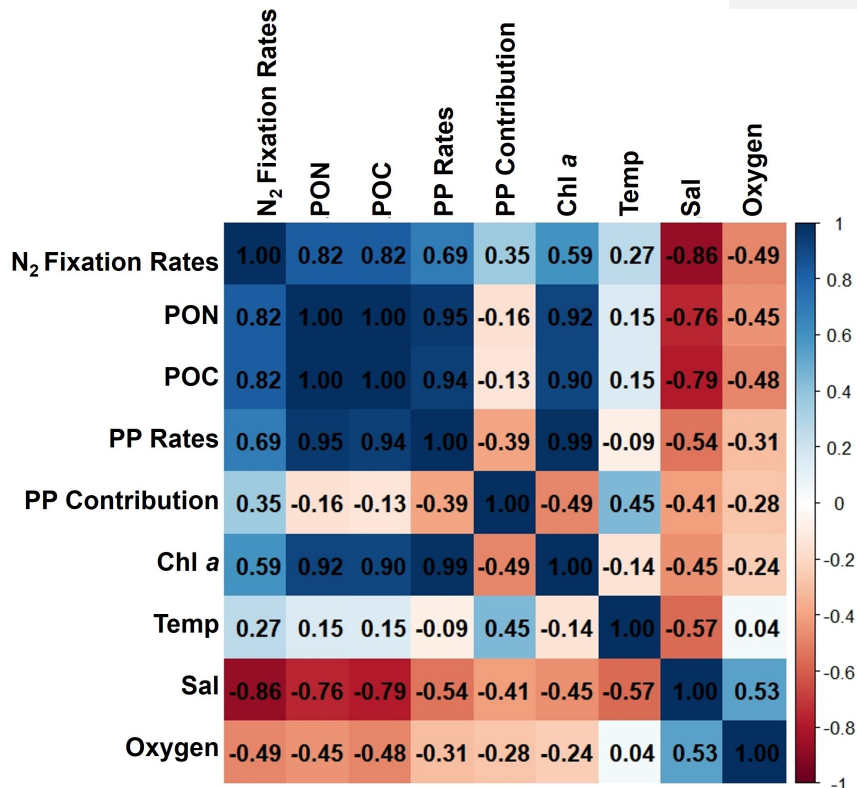
Deleted: ?;

877 Qeqertarsuaq's future hydrographic state. By detailing the environmental and hydrographic  
878 changes, we contribute valuable knowledge to the broader context of N<sub>2</sub> fixation in the Arctic  
879 Ocean. Given nitrogen's pivotal role in Arctic ecosystem productivity, it is essential to explore  
880 diazotrophs, quantify N<sub>2</sub> fixation, and assess their impact on ecosystem services as climate change  
881 progresses.

882 **Appendix A**

883  
884



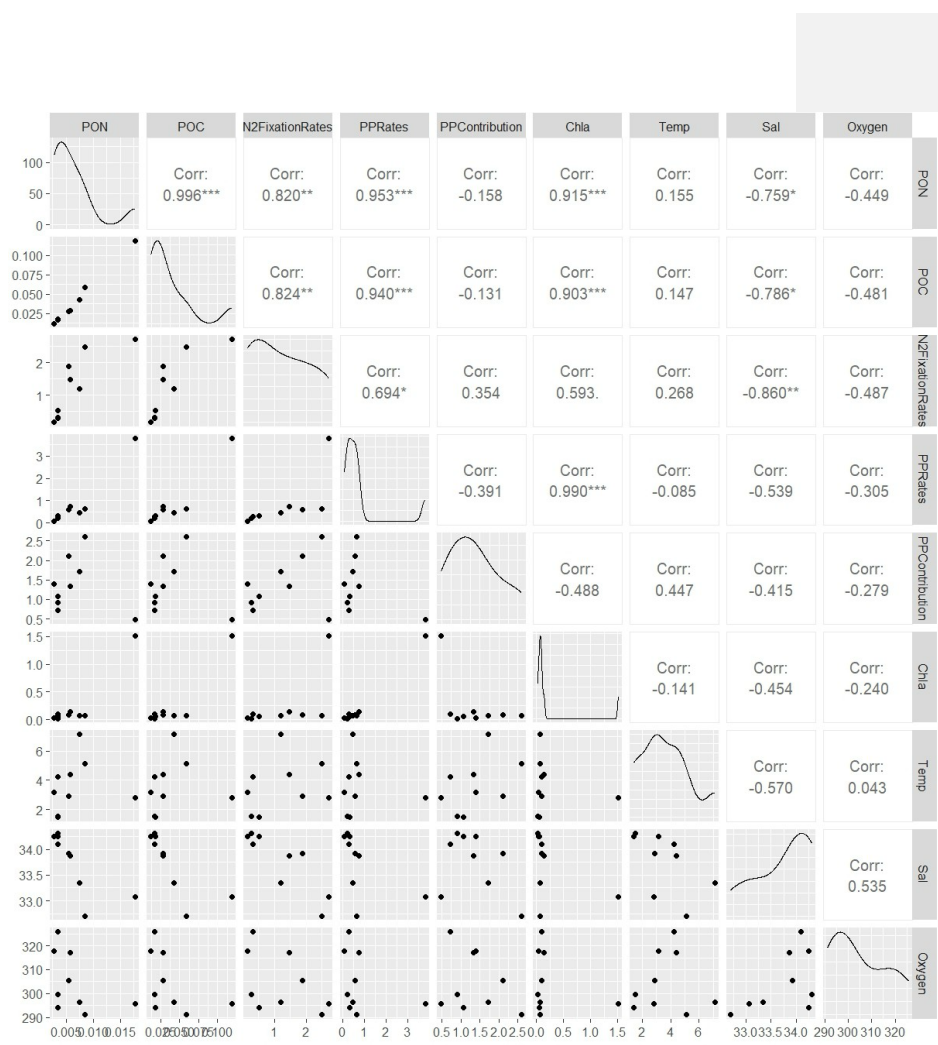


891

892

893

**Figure A2.** Correlation matrix of environmental and biological variables. The plot shows the correlation coefficients between the following parameters: N<sub>2</sub> fixation rates, PON, POC, PP rates, the contribution N<sub>2</sub> fixation to PP (PP contribution), Chl a, temperature (Temp), salinity (Sal), and Oxygen. The scale ranges from -1 to 1, where values close to 1 or -1 indicate strong positive or negative correlations, respectively, and values near 0 indicate weak or no correlation. The color intensity represents the strength and direction of the correlations, facilitating the identification of relationships among the variables



899

900

901 **Figure A3.** This figure displays a ggpairs plot, showing pairwise relationships and correlations between  
 902 biological and environmental variables. Pearson correlation coefficients displayed in the upper triangular  
 903 panel, indicating the strength and significance of linear relationships. Statistical significance levels are  
 904 indicated by stars (\*), where \* indicates  $p < 0.05$ , \*\* indicates  $p < 0.01$  and \*\*\* indicates  $p < 0.001$

905

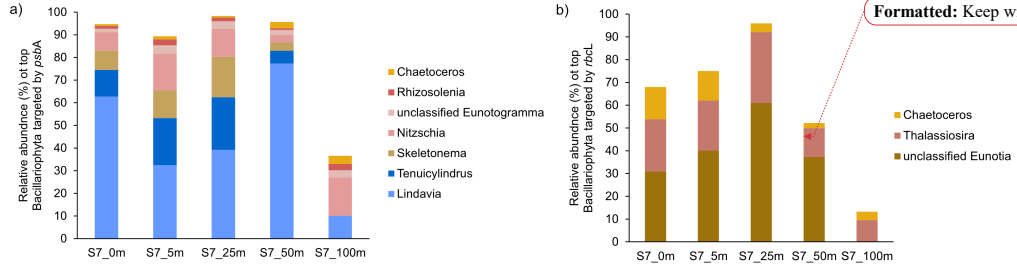
906  
907  
908909  
910  
911  
912

Figure A4 . Taxonomic composition of Bacillariophyta at Station 7 based on a) psbA and b) rbcL marker genes. The figure shows the relative abundance of Bacillariophyta genera detected in the metagenomic dataset, grouped by gene-specific classifications.

913

Station	Parameter (X)	Value	SD	$\delta NFR/\delta X$	Error contribution ( $SD_x/ \delta NFR/\delta X $ ) <sup>2</sup>	% Total error	Summary (nmol N L <sup>-1</sup> d <sup>-1</sup> )
3	$\Delta t$	1.00	0.00	0.00	0.00	0.00	Mean = 1.13 LOD = 0.73 MQR = 0.12
	$A_{N2}$	3.92%	0.00	0.00	0.00	0.00	
	$A_{PN0}$	0.370%	$4.24 \times 10^{-6}$	$2.63 \times 10^2$	$2.46 \times 10^2$	29.49	
	$A_{PNf}$	0.420%	$3.7 \times 10^{-5}$	$2.36 \times 10^5$	$3.03 \times 10^2$	35.54	
	$[PN]_f$	$1.69 \times 10^3$	$1.24 \times 10^2$	$5.12 \times 10^2$	$3.21 \times 10^2$	34.97	
7	$\Delta t$	1.00	0.00	0.00	0.00	0.00	Mean = 1.92 LOD =

Formatted: Keep with next

Formatted: Font: 9 pt, Bold, Font colour: Text 2

Formatted: Font: Not Bold

Formatted: Font: Not Bold, Italic

Formatted: Normal, Left

							<u>1.91</u> <u>MQR =</u> <u>0.47</u>
	<u>A<sub>N2</sub></u>	<u>3.92%</u>	<u>0.00</u>	<u>0.00</u>	<u>0.00</u>	<u>0.00</u>	
	<u>A<sub>PNO</sub></u>	<u>0.369%</u>	<u>4.0</u> <u>x 10<sup>-6</sup></u>	<u>1.57 x</u> <u>10<sup>7</sup></u>	<u>2.06 x 10<sup>3</sup></u>	<u>25.17</u>	
	<u>A<sub>PNF</sub></u>	<u>0.407%</u>	<u>5.47</u> <u>x 10<sup>-5</sup></u>	<u>9.25 x</u> <u>10<sup>5</sup></u>	<u>2.79 x 10<sup>3</sup></u>	<u>36.88</u>	
	<u>[PN]<sub>f</sub></u>	<u>4.62 x</u> <u>10<sup>3</sup></u>	<u>8.2</u> <u>x</u> <u>10<sup>2</sup></u>	<u>6.77 x</u> <u>10<sup>2</sup></u>	<u>2.87 x 10<sup>3</sup></u>	<u>37.95</u>	
10	<u>Δt</u>	<u>1.00</u>	<u>0.00</u>	<u>0.00</u>	<u>0.00</u>	<u>0.00</u>	<u>Mean =</u> <u>0.90</u> <u>LOD =</u> <u>0.96</u> <u>MQR =</u> <u>0.06</u>
	<u>A<sub>N2</sub></u>	<u>3.92%</u>	<u>0.00</u>	<u>0.00</u>	<u>0.00</u>	<u>0.00</u>	
	<u>A<sub>PNO</sub></u>	<u>0.371%</u>	<u>1.89</u> <u>x 10<sup>-6</sup></u>	<u>-2.01 x</u> <u>10<sup>2</sup></u>	<u>1.44 x 10<sup>-3</sup></u>	<u>31.24</u>	
	<u>A<sub>PNF</sub></u>	<u>0.371%</u>	<u>2.22</u> <u>x 10<sup>-6</sup></u>	<u>2.01 x</u> <u>10<sup>2</sup></u>	<u>2.05 x 10<sup>-3</sup></u>	<u>34.85</u>	
	<u>[PN]<sub>f</sub></u>	<u>5.91 x</u> <u>10<sup>2</sup></u>	<u>1.89</u> <u>x</u> <u>10<sup>2</sup></u>	<u>-1.56 x</u> <u>10<sup>-4</sup></u>	<u>3.69 x 10<sup>-3</sup></u>	<u>33.91</u>	

914 *Table A1: Sensitivity analysis for N<sub>2</sub> fixation rates. The contribution of each source of error to the total*  
915 *uncertainty was determined and calculated after Montoya et al., (1996). Average values and standard deviations*  
916 *(SD) are provided for all parameters at each station. The partial derivative ( $\partial NFR / \partial X$ ) of the N<sub>2</sub> fixation rate*  
917 *measurements is calculated for each parameter and evaluated using the provided average and standard*  
918 *deviation. The total and relative error are given for each parameter. Mean represents the average N<sub>2</sub> fixation*  
919 *rate measurement. MQR (minimal quantifiable rate) represents the total uncertainty linked to every measurement*  
920 *and is calculated using standard propagation of error. LOD (limit of detection) represents an alternative*  
921 *detection limit defined as AAPN = 0.00146.*

922  
923 *Data availability.* The presented data collected during the cruise will be made accessible on PANGEA. The  
924 molecular datasets have been deposited with the accession number: Bioproject PRJNA1133027.

925  
926  
927 *Author contributions.* IS carried out fieldwork and laboratory work at the University of Southern Denmark,  
928

← Formatted: Keep with next

← Formatted: Caption

Deleted: Bioproject PRJNA1133027.

930 and wrote the majority of the manuscript. ELP, AM, and EL conducted fieldwork and laboratory work at the  
931 University of Southern Denmark. PX performed metagenomic analysis and created the corresponding graphs.  
932 CRL designed the study, provided supervision and guidance throughout the project, and contributed to the  
933 writing and revision of the manuscript. All authors contributed to the conception of the study and participated  
934 in the writing and revision of the manuscript.

935  
936  
937  
938 *Competing interests.* The authors declare that they have no known competing financial interests or personal  
939 relationships that could have appeared to influence the work reported in this paper. One of the authors, CRL,  
940 serves as an Associate Editor for Biogeosciences.

941  
942  
943  
944 *Acknowledgements.* This work was supported by the Velux Foundation (grant no.29411 to Carolin R.  
945 Löscher) and through the DFF grant from the the Independent Research Fund Denmark (grant no. 0217-  
946 00089B to Lasse Riemann, Carolin R. Löscher and Stig Markager). ELP was supported by a postdoctoral  
947 contract from Danmarks Frie Forskningsfond (DFF, 1026-00428B) at SDU, and by a Marie Skłodowska-  
948 Curie postdoctoral fellowship (HORIZON291 MSCA-2021-PF-01, project number: 101066750) by the  
949 European Commission at Princeton University. We sincerely thank the captain and crew of the P540 during the  
950 cruise on the Danish military vessel for their invaluable support and cooperation at sea. Our gratitude extends  
951 to Isaaffik Arctic Gateway for providing the infrastructure and opportunities that made this project possible.  
952 We also acknowledge Zarah Kofod for her technical support in the laboratory and thank all the Nordceo  
953 laboratory technicians for their general assistance.

954 **References**

955  
956 Ardyna, M. and Arrigo, K. R.: Phytoplankton dynamics in a changing Arctic Ocean, *Nature Climate Change*, 10,  
957 892–903, 2020.  
958 Ardyna, M., Babin, M., Gosselin, M., Devred, E., Rainville, L., and Tremblay, J.-É.: Recent Arctic Ocean  
959 sea ice loss triggers novel fall phytoplankton blooms, *Geophysical Research Letters*, 41, 6207–6212,  
960 2014.  
961 Arrigo, K. R. and van Dijken, G. L.: Continued increases in Arctic Ocean primary production, *Progress in  
962 oceanography*, 136, 60–70, 2015. Arrigo, K. R., van Dijken, G., and Pabi, S.: Impact of a shrinking Arctic  
963 ice cover on marine primary production, *Geophysical Research  
964 Letters*, 35, 2008.  
965 Arrigo, K. R., van Dijken, G. L., Castelao, R. M., Luo, H., Rennermalm, Å. K., Tedesco, M., Mote, T. L.,  
966 Oliver, H., and Yager, P. L.: Melting glaciers stimulate large summer phytoplankton blooms in southwest  
967 Greenland waters, *Geophysical Research Letters*, 44, 6278– 6285, 2017.  
968 Bhatia, M. P., Kujawinski, E. B., Das, S. B., Breier, C. F., Henderson, P. B., and Charette, M. A.: Greenland  
969 meltwater as a significant and potentially bioavailable source of iron to the ocean, *Nature Geoscience*, 6,

274–278, 2013.

Blais, M., Tremblay, J.-É., Jungblut, A. D., Gagnon, J., Martin, J., Thaler, M., and Lovejoy, C.: Nitrogen fixation and identification of potential diazotrophs in the Canadian Arctic, *Global Biogeochemical Cycles*, 26, 2012.

Bonnet, S., Biegala, I. C., Dutrieux, P., Slemmons, L. O., and Capone, D. G.: Nitrogen fixation in the western equatorial Pacific: Rates, diazotrophic cyanobacterial size class distribution, and biogeochemical significance, *Global Biogeochemical Cycles*, 23, 2009.

Buchanan, P. J., Chase, Z., Matear, R. J., Phipps, S. J., and Bindoff, N. L.: Marine nitrogen fixers mediate a low latitude pathway for atmospheric CO<sub>2</sub> drawdown, *Nature Communications*, 10, 4611, 2019.

Cantalapiedra, C. P., Hernández-Plaza, A., Letunic, I., Bork, P., and Huerta-Cepas, J.: eggNOG-mapper v2: functional annotation, orthology assignments, and domain prediction at the metagenomic scale, *Molecular biology and evolution*, 38, 5825–5829, 2021.

Capone, D. G. and Carpenter, E. J.: Nitrogen fixation in the marine environment, *Science*, 217, 1140–1142, 1982.

Chen, Y., Chen, Y., Shi, C., Huang, Z., Zhang, Y., Li, S., Li, Y., Ye, J., Yu, C., Li, Z., et al.: SOAPnuke: a MapReduce acceleration-supported software for integrated quality control and preprocessing of high-throughput sequencing data, *Gigascience*, 7, gix120, 2018.

Cheung, S., Liu, K., Turk-Kubo, K. A., Nishioka, J., Suzuki, K., Landry, M. R., Zehr, J. P., Leung, S., Deng, L., and Liu, H.: High biomass turnover rates of endosymbiotic nitrogen-fixing cyanobacteria in the western Bering Sea, *Limnology and Oceanography Letters*, 7, 501–509, 2022.

Coale, T. H., Loconte, V., Turk-Kubo, K. A., Vanslembrouck, B., Mak, W. K. E., Cheung, S., Ekman, A., Chen, J.-H., Hagino, K., Takano, Y., et al.: Nitrogen-fixing organelle in a marine alga, *Science*, 384, 217–222, 2024.

Dähnke, K. and Thamdrup, B.: Nitrogen isotope dynamics and fractionation during sedimentary denitrification in Boknafjord, Baltic Sea, *Biogeosciences*, 10, 3079–3088, 2013.

Damm, E., Helmke, E., Thoms, S., Schauer, U., Nöthig, E., Bakker, K., and Kiene, R.: Methane production in aerobic oligotrophic surface water in the central Arctic Ocean, *Biogeosciences*, 7, 1099–1108, 2010.

Díez, B., Bergman, B., Pedrós-Alió, C., Antó, M., and Snoeijs, P.: High cyanobacterial *nifH* gene diversity in Arctic seawater and sea ice brine, *Environmental microbiology reports*, 4, 360–366, 2012.

Emeis, K.-C., Mara, P., Schlarbaum, T., Möbius, J., Dähnke, K., Struck, U., Mihalopoulos, N., and Krom, M.: External N inputs and internal N cycling traced by isotope ratios of nitrate, dissolved reduced nitrogen, and particulate nitrogen in the eastern Mediterranean Sea, *Journal of Geophysical Research: Biogeosciences*, 115, 2010.

Falkowski, P. G., Fenchel, T., and Delong, E. F.: The microbial engines that drive Earth's biogeochemical cycles, *science*, 320, 1034–1039, 2008.

Farnelid, H., Andersson, A. F., Bertilsson, S., Al-Soud, W. A., Hansen, L. H., Sørensen, S., Steward, G. F., Hagström, Å., and Riemann, L.: Nitrogenase gene amplicons from global marine surface waters are dominated by genes of non-cyanobacteria, *PloS one*, 6, e19223, 2011.

1007 Farnelid, H., Turk-Kubo, K., Ploug, H., Ossolinski, J. E., Collins, J. R., Van Mooy, B. A., and Zehr, J. P.:  
 1008 Diverse diazotrophs are present on sinking particles in the North Pacific Subtropical Gyre, *The ISME*  
 1009 journal, 13, 170–182, 2019.

1010 Fernández-Méndez, M., Turk-Kubo, K. A., Buttigieg, P. L., Rapp, J. Z., Krumpen, T., and Zehr, J. P.:  
 1011 Diazotroph diversity in the sea ice, melt ponds, and surface waters of the Eurasian Basin of the Central  
 1012 Arctic Ocean, *Frontiers in microbiology*, 7, 217 140, 2016.

1013 [Foster, R. A., Goebel, N. L., & Zehr, J. P.: Isolation of \*calothrix rhizosoleniae\* \(cyanobacteria\) strain SC01](#)  
 1014 [from \*chaetoceros\* \(bacillariophyta\) spp. diatoms of the subtropical north pacific ocean 1. \*Journal of\*](#)  
 1015 [Phycology](#), 46(5), 1028-1037, 2010.

1016 Foster, R. A., Kuypers, M. M., Vagner, T., Paerl, R. W., Musat, N., and Zehr, J. P.: Nitrogen fixation and  
 1017 transfer in open ocean diatom– cyanobacterial symbioses, *The ISME journal*, 5, 1484–1493, 2011.

1018 Foster, R. A., Tienken, D., Littmann, S., Whitehouse, M. J., Kuypers, M. M., and White, A. E.: The rate and  
 1019 fate of N2 and C fixation by marine diatom-diazotroph symbioses, *The ISME journal*, 16, 477–487, 2022.

1020 Fox, A. and Walker, B. D.: Sources and Cycling of Particulate Organic Matter in Baffin Bay: A Multi-Isotope  
 1021  $\delta^{13}\text{C}$ ,  $\delta^{15}\text{N}$ , and  $\Delta^{14}\text{C}$   
 1022 Approach, *Frontiers in Marine Science*, 9, 846 025, 2022.

1023 Fu, L., Niu, B., Zhu, Z., Wu, S., and Cd-hit, W. L.: Accelerated for clustering the next-generation  
 1024 sequencing data, *Bioinformatics*, 28, 3150–3152, 2012.

1025 Galloway, J., Dentener, F., Capone, D., Boyer, E., Howarth, R., Seitzinger, S., Asner, G., Cleveland, C., Green,  
 1026 P., Holland, E., et al.: Nitrogen cycles: past, present, and future. *Biogeochemistry* 70, 153e226, 2004.

1027 García-Robledo, E., Corzo, A., and Papaspyrou, S.: A fast and direct spectrophotometric method for the  
 1028 sequential determination of nitrate and nitrite at low concentrations in small volumes, *Marine Chemistry*,  
 1029 162, 30–36, 2014.

1030 [Geider, R. J., & La Roche, J.: Redfield revisited: variability of C \[ratio\] N \[ratio\] P in marine microalgae and](#)  
 1031 [its biochemical](#)  
 1032 [basis. \*European Journal of Phycology\*, 37\(1\), 1-17, 2002.](#)

1033 Gladish, C. V., Holland, D. M., and Lee, C. M.: Oceanic boundary conditions for Jakobshavn Glacier. Part  
 1034 II: Provenance and sources of variability of Disko Bay and Ilulissat icefjord waters, 1990–2011, *Journal*  
 1035 of *Physical Oceanography*, 45, 33–63, 2015.

1036 [Grosse, J., Bombar, D., Doan, H. N., Nguyen, L. N., & Voss, M.: The Mekong River plume fuels nitrogen](#)  
 1037 [fixation and determines phytoplankton species distribution in the South China Sea during low and high](#)  
 1038 [discharge season. \*Limnology and Oceanography\*, 55\(4\), 1668-1680, 2010.](#)

1039 Großkopf, T., Mohr, W., Baustian, T., Schunck, H., Gill, D., Kuypers, M. M., Lavik, G., Schmitz, R. A.,  
 1040 Wallace, D. W., and LaRoche, J.: Doubling of marine dinitrogen-fixation rates based on direct  
 1041 measurements, *Nature*, 488, 361–364, 2012.

1042 Gruber, N.: The dynamics of the marine nitrogen cycle and its influence on atmospheric CO<sub>2</sub> variations, in:  
 1043 The ocean carbon cycle and climate, pp. 97–148, Springer, 2004.

1044 Gruber, N. and Galloway, J. N.: An Earth-system perspective of the global nitrogen cycle, *Nature*, 451, 293–296,

Formatted: English (UK)

Formatted: Indent: Left: 0,14 cm, First line: 0 cm

Formatted: Font: Not Italic

Formatted: Font: Not Italic

Formatted

1045 2008.

1046 Gruber, N. and Sarmiento, J. L.: Global patterns of marine nitrogen fixation and denitrification, *Global*  
1047 *biogeochemical cycles*, 11, 235–266, 1997.

1048 Haine, T. W., Curry, B., Gerdes, R., Hansen, E., Karcher, M., Lee, C., Rudels, B., Spreen, G., de Steur, L.,  
1049 Stewart, K. D., et al.: Arctic freshwater export: Status, mechanisms, and prospects, *Global and Planetary*  
1050 *Change*, 125, 13–35, 2015.

1051 Hanna, E., Huybrechts, P., Steffen, K., Cappelen, J., Huff, R., Shuman, C., Irvine-Fynn, T., Wise, S., and  
1052 Griffiths, M.: Increased runoff from melt from the Greenland Ice Sheet: a response to global warming,  
1053 *Journal of Climate*, 21, 331–341, 2008.

1054 Hansen, M. O., Nielsen, T. G., Stedmon, C. A., and Munk, P.: Oceanographic regime shift during 1997 in  
1055 Disko Bay, western Greenland, *Limnology and Oceanography*, 57, 634–644, 2012.

1056 Harding, K., Turk-Kubo, K. A., Sipler, R. E., Mills, M. M., Bronk, D. A., and Zehr, J. P.: Symbiotic  
1057 unicellular cyanobacteria fix nitrogen in the Arctic Ocean, *Proceedings of the National Academy of*  
1058 *Sciences*, 115, 13 371–13 375, 2018.

1059 Hawkings, J., Wadham, J., Tranter, M., Lawson, E., Sole, A., Cowton, T., Tedstone, A., Bartholomew, I.,  
1060 Nienow, P., Chandler, D., et al.: The effect of warming climate on nutrient and solute export from the  
1061 Greenland Ice Sheet, *Geochemical Perspectives Letters*, pp. 94–104, 2015.

1062 Hawkings, J. R., Wadham, J. L., Tranter, M., Raiswell, R., Benning, L. G., Statham, P. J., Tedstone, A.,  
1063 Nienow, P., Lee, K., and Telling, J.: Ice sheets as a significant source of highly reactive nanoparticulate  
1064 iron to the oceans, *Nature communications*, 5, 1–8, 2014.

1065 Hendry, K. R., Huvenne, V. A., Robinson, L. F., Annett, A., Badger, M., Jacobel, A. W., Ng, H. C., Opher, J.,  
1066 Pickering, R. A., Taylor, M. L., et al.: The biogeochemical impact of glacial meltwater from Southwest  
1067 Greenland, *Progress in Oceanography*, 176, 102 126, 2019.

1068 Holland, D. M., Thomas, R. H., De Young, B., Ribergaard, M. H., and Lyberth, B.: Acceleration of  
1069 Jakobshavn Isbræ triggered by warm subsurface ocean waters, *Nature geoscience*, 1, 659–664, 2008.

1070 Hopwood, M. J., Connelly, D. P., Arendt, K. E., Juul-Pedersen, T., Stinchcombe, M. C., Meire, L., Esposito,  
1071 M., and Krishna, R.: Seasonal changes in Fe along a glaciated Greenlandic fjord, *Frontiers in Earth*  
1072 *Science*, 4, 15, 2016.

1073 Hyatt, D., Chen, G.-L., LoCascio, P. F., Land, M. L., Larimer, F. W., and Hauser, L. J.: Prodigal: prokaryotic  
1074 gene recognition and translation initiation site identification, *BMC bioinformatics*, 11, 1–11, 2010.

1075 Jensen, H. M., Pedersen, L., Burmeister, A., and Winding Hansen, B.: Pelagic primary production during  
1076 summer along 65 to 72 N off West Greenland, *Polar Biology*, 21, 269–278, 1999.

1077 Karl, D., Michaels, A., Bergman, B., Capone, D., Carpenter, E., Letelier, R., Lipschultz, F., Paerl, H.,  
1078 Sigman, D., and Stal, L.: Dinitrogen fixation in the world's oceans, *The nitrogen cycle at regional to global*  
1079 *scales*, pp. 47–98, 2002.

1080 Kries, J.: Nitrogen isotope evidence for changing Arctic Ocean ventilation regimes during the Cenozoic,  
1081 *Geophysical Research Letters*, 49, e2022GL099 512, 2022.

1082 Krawczyk, D. W., Yesson, C., Knutz, P., Arboe, N. H., Blicher, M. E., Zinglersen, K. B., and Wagnholt, J.  
1083 N.: Seafloor habitats across geological boundaries in Disko Bay, central West Greenland, *Estuarine, Coastal and Shelf Science*, 278, 108 087, 2022.

1084 Krupke, A., Mohr, W., LaRoche, J., Fuchs, B. M., Amann, R. I., and Kuypers, M. M.: The effect of nutrients  
1085 on carbon and nitrogen fixation by the UCYN-A–haptophyte symbiosis, *The ISME journal*, 9, 1635–1647,  
1086 2015.

1087 Laso Perez, R., Rivas Santisteban, J., Fernandez-Gonzalez, N., Mundy, C. J., Tamames, J., and Pedros-Alio,  
1088 C.: Nitrogen cycling during an Arctic bloom: from chemolithotrophy to nitrogen assimilation, *bioRxiv*,  
1089 pp. 2024–02, 2024.

1090 Lewis, K., Van Dijken, G., and Arrigo, K. R.: Changes in phytoplankton concentration now drive increased  
1091 Arctic Ocean primary production, *Science*, 369, 198–202, 2020.

1092 Li, D., Liu, C.-M., Luo, R., Sadakane, K., and Lam, T.-W.: MEGAHit: an ultra-fast single-node solution for  
1093 large and complex metagenomics assembly via succinct de Bruijn graph, *Bioinformatics*, 31, 1674–1676,  
1094 2015.

1095 Lüscher, C. R., Bourbonnais, A., Dekaezemacker, J., Charoenpong, C. N., Altabet, M. A., Bange, H. W.,  
1096 Czeschel, R., Hoffmann, C., and Schmitz, R.: N<sub>2</sub> fixation in eddies of the eastern tropical South Pacific  
1097 Ocean, *Biogeosciences*, 13, 2889–2899, 2016.

1098 Lüscher, C. R., Mohr, W., Bange, H. W., and Canfield, D. E.: No nitrogen fixation in the Bay of Bengal?,  
1099 *Biogeosciences*, 17, 851–864, 2020. Luo, Y.-W., Doney, S., Anderson, L., Benavides, M., Berman-Frank, I.,  
1100 Bode, A., Bonnet, S., Boström, K. H., Böttjer, D., Capone, D., et al.: Database of diazotrophs in global ocean:  
1101 abundance, biomass and nitrogen fixation rates, *Earth System Science Data*, 4, 47–73, 2012.

1102 Martínez-Pérez, C., Mohr, W., Lüscher, C. R., Dekaezemacker, J., Littmann, S., Yilmaz, P., Lehnen, N.,  
1103 Fuchs, B. M., Lavik, G., Schmitz,  
1104 R. A., et al.: The small unicellular diazotrophic symbiont, UCYN-A, is a key player in the marine nitrogen  
1105 cycle, *Nature Microbiology*, 1, 1–7, 2016.

1106 Mills, M. M., Turk-Kubo, K. A., van Dijken, G. L., Henke, B. A., Harding, K., Wilson, S. T., Arrigo, K. R.,  
1107 and Zehr, J. P.: Unusual marine cyanobacteria/haptophyte symbiosis relies on N<sub>2</sub> fixation even in N-rich  
1108 environments, *The ISME Journal*, 14, 2395–2406, 2020.

1109 Mohr, W., Grosskopf, T., Wallace, D. W., and LaRoche, J.: Methodological underestimation of oceanic  
1110 nitrogen fixation rates, *PLoS one*, 5, e12 583, 2010.

1111 Montoya, J. P.: Nitrogen stable isotopes in marine environments, *Nitrogen in the marine environment*, 2, 1277–  
1112 1302, 2008.

1113 Montoya, J. P., Carpenter, E. J., and Capone, D. G.: Nitrogen fixation and nitrogen isotope abundances in  
1114 zooplankton of the oligotrophic North Atlantic, *Limnology and Oceanography*, 47, 1617–1628, 2002.

1115 Mortensen, J., Rysgaard, S., Winding, M., Juul-Pedersen, T., Arendt, K., Lund, H., Stuart-Lee, A., and Meire,  
1116 L.: Multidecadal water mass dynamics on the West Greenland Shelf, *Journal of Geophysical Research: Oceans*, 127, e2022JC018 724, 2022.

1117 Munk, P., Nielsen, T. G., and Hansen, B. W.: Horizontal and vertical dynamics of zooplankton and larval  
1118

1119

1120 fish communities during mid- summer in Disko Bay, West Greenland, *Journal of Plankton Research*, 37,  
1121 554–570, 2015.

1122 Murphy, J. and Riley, J. P.: A modified single solution method for the determination of phosphate in natural  
1123 waters, *Analytica chimica acta*, 27, 31–36, 1962.

1124 Myers, P. G. and Ribergaard, M. H.: Warming of the polar water layer in Disko Bay and potential impact on  
1125 Jakobshavn Isbrae, *Journal of Physical Oceanography*, 43, 2629–2640, 2013.

1126 Patro, R., Duggal, G., Love, M. I., Irizarry, R. A., and Kingsford, C.: Salmon provides fast and bias-aware  
1127 quantification of transcript expression, *Nature methods*, 14, 417–419, 2017.

1128 Quigg, A., Finkel, Z.V., Irwin, A.J., Rosenthal, Y., Ho, T.Y., Reinfelder, J.R., Schofield, O., Morel, F.M.,  
1129 and Falkowski, P.G.: The evolutionary inheritance of elemental stoichiometry in marine  
1130 phytoplankton, *Nature*, 425(6955), pp.291–294, 2003.

1131 Redfield, A. C.: *On the proportions of organic derivatives in sea water and their relation to the composition  
1132 of plankton (Vol. 1)*. Liverpool: university press of liverpool, 1934.

1133 Reeder, C. F., Stoltenberg, I., Javidpour, J., and Löscher, C. R.: Salinity as a key control on the diazotrophic  
1134 community composition in the Baltic Sea, *Ocean Science Discussions*, 2021, 1–30, 2021.

1135 Rees, A. P., Gilbert, J. A., and Kelly-Gerrey, B. A.: Nitrogen fixation in the western English Channel (NE  
1136 Atlantic ocean), *Marine Ecology Progress Series*, 374, 7–12, 2009.

1137 Robicheau, B. M., Tolman, J., Rose, S., Desai, D., and LaRoche, J.: Marine nitrogen-fixers in the Canadian  
1138 Arctic Gateway are dominated by biogeographically distinct noncyanobacterial communities, *FEMS  
1139 Microbiology Ecology*, 99(12), 122, 2023.

1140 Rysgaard, S., Boone, W., Carlson, D., Sejr, M., Bendtsen, J., Juul-Pedersen, T., Lund, H., Meire, L., and  
1141 Mortensen, J.: An updated view on water masses on the pan-west Greenland continental shelf and their  
1142 link to proglacial fjords, *Journal of Geophysical Research: Oceans*, 125, e2019JC015 564, 2020.

1143 Schiøtt, S.: The Marine Ecosystem of Ilulissat Icefjord, Greenland, Ph.D. thesis, Department of Biology,  
1144 Aarhus University, Denmark, 2023. Schlitzer, R.: Ocean data view, 2022.

1145 Schneider, B., Schlitzer, R., Fischer, G. and Nöthig, E.M.: Depth-dependent elemental compositions of  
1146 particulate organic matter (POM) in the ocean, *Global Biogeochemical Cycles*, 17(2), 2003.

1147 Schvarcz, C. R., Wilson, S. T., Caffin, M., Stancheva, R., Li, Q., Turk-Kubo, K. A., White, A. E., Karl, D. M.,  
1148 Zehr, J. P., and Steward, G. F.: Overlooked and widespread pennate diatom-diazotroph symbioses in the  
1149 sea, *Nature communications*, 13, 799, 2022.

1150 Shao, Z., Xu, Y., Wang, H., Luo, W., Wang, L., Huang, Y., Agawin, N. S. R., Ahmed, A., Benavides, M.,  
1151 Bentzon-Tilia, M., et al.: Global oceanic diazotroph database version 2 and elevated estimate of global N  
1152 fixation, *Earth System Science Data*, 15, 2023.

1153 Sherwood, O. A., Davin, S. H., Lehmann, N., Buchwald, C., Edinger, E. N., Lehmann, M. F., and Kienast,  
1154 M.: Stable isotope ratios in seawater nitrate reflect the influence of Pacific water along the northwest  
1155 Atlantic margin, *Biogeosciences*, 18, 4491–4510, 2021.

1156 Shiozaki, T., Bombar, D., Riemann, L., Hashihama, F., Takeda, S., Yamaguchi, T., Ehama, M., Hamasaki,  
1157 K., and Furuya, K.: Basin scale variability of active diazotrophs and nitrogen fixation in the North Pacific,

1158 from the tropics to the subarctic Bering Sea, *Global Biogeochemical Cycles*, 31, 996–1009, 2017.

1159 Shiozaki, T., Fujiwara, A., Ijichi, M., Harada, N., Nishino, S., Nishi, S., Nagata, T., and Hamasaki, K.:  
1160 Diazotroph community structure and the role of nitrogen fixation in the nitrogen cycle in the Chukchi Sea  
1161 (western Arctic Ocean), *Limnology and Oceanography*, 63, 2191–2205, 2018.

1162 Shiozaki, T., Fujiwara, A., Inomura, K., Hirose, Y., Hashihama, F., and Harada, N.: Biological nitrogen  
1163 fixation detected under Antarctic sea ice, *Nature geoscience*, 13, 729–732, 2020.

1164 Shiozaki, T., Nishimura, Y., Yoshizawa, S., Takami, H., Hamasaki, K., Fujiwara, A., Nishino, S., and Harada,  
1165 N.: Distribution and survival strategies of endemic and cosmopolitan diazotrophs in the Arctic Ocean, *The  
1166 ISME journal*, 17, 1340–1350, 2023.

1167 Sigman, D. M., DiFiore, P. J., Hain, M. P., Deutsch, C., Wang, Y., Karl, D. M., Knapp, A. N., Lehmann, M.  
1168 F., and Pantoja, S.: The dual isotopes of deep nitrate as a constraint on the cycle and budget of oceanic  
1169 fixed nitrogen, *Deep Sea Research Part I: Oceanographic Research Papers*, 56, 1419–1439, 2009.

1170 Sipler, R. E., Gong, D., Baer, S. E., Sanderson, M. P., Roberts, Q. N., Mulholland, M. R., and Bronk, D. A.:  
1171 Preliminary estimates of the contribution of Arctic nitrogen fixation to the global nitrogen budget,  
1172 *Limnology and Oceanography Letters*, 2, 159–166, 2017.

1173 Slawyk, G., Collos, Y., and Auclair, J.-C.: The use of the  $^{13}\text{C}$  and  $^{15}\text{N}$  isotopes for the simultaneous  
1174 measurement of carbon and nitrogen turnover rates in marine phytoplankton 1, *Limnology and  
1175 Oceanography*, 22, 925–932, 1977.

1176 Sohm, J. A., Webb, E. A., and Capone, D. G.: Emerging patterns of marine nitrogen fixation, *Nature Reviews  
1177 Microbiology*, 9, 499–508, 2011.

1178 Stern, R. W., & Elser, J. J. *Ecological stoichiometry: the biology of elements from molecules to the biosphere*.  
1179 In: *Ecological stoichiometry*. Princeton university press, 2017.

1180 Tanioka, T., Garcia, C.A., Larkin, A.A., Garcia, N.S., Fagan, A.J. and Martiny, A.C.: Global patterns and  
1181 predictors of C: N: P in marine ecosystems, *Communications Earth & Environment*, 3(1), p.271, 2022.

1182 Tang, W., Wang, S., Fonseca-Batista, D., Dehairs, F., Gifford, S., Gonzalez, A. G., Gallinari, M., Planquette,  
1183 H., Sarthou, G., and Cassar, N.: Revisiting the distribution of oceanic N2 fixation and estimating  
1184 diazotrophic contribution to marine production, *Nature communications*, 10, 831, 2019.

1185 Tremblay, J.-É. and Gagnon, J.: The effects of irradiance and nutrient supply on the productivity of Arctic  
1186 waters: a perspective on climate change, in: *Influence of climate change on the changing arctic and sub-  
1187 arctic conditions*, pp. 73–93, Springer, 2009.

1188 Turk, K. A., Rees, A. P., Zehr, J. P., Pereira, N., Swift, P., Shelley, R., Lohan, M., Woodward, E. M. S., and  
1189 Gilbert, J.: Nitrogen fixation and nitrogenase (nifH) expression in tropical waters of the eastern North  
1190 Atlantic, *The ISME journal*, 5, 1201–1212, 2011.

1191 Turk-Kubo, K. A., Frank, I. E., Hogan, M. E., Desnues, A., Bonnet, S., and Zehr, J. P.: Diazotroph community  
1192 succession during the VAHINE mesocosm experiment (New Caledonia lagoon), *Biogeosciences*, 12,  
1193 7435–7452, 2015.

1194 Von Friesen, L. W. and Riemann, L.: Nitrogen fixation in a changing Arctic Ocean: an overlooked source of

**Formatted:** Font: Not Italic

**Formatted:** Font: Not Italic

**Formatted:** Font: Not Italic

**Formatted:** Condensed by 0,1 pt

1195      nitrogen? *Frontiers in Microbiology*, 11, 596 426, 2020.

1196      Wang, S., Bailey, D., Lindsay, K., Moore, J., and Holland, M.: Impact of sea ice on the marine iron cycle

1197      and phytoplankton productivity, *Biogeosciences*, 11, 4713–4731, 2014.

1198      Zehr, J. P. and Capone, D. G.: Changing perspectives in marine nitrogen fixation, *Science*, 368, eaay9514, 2020.

Formatted: Condensed by 0,1 pt

|

x

Formatted

[... [2]]